

UNIVERSITÀ
DEGLI STUDI
DI PADOVA

Sede Amministrativa: **Università degli Studi di Padova**

Dipartimento di GEOSCIENZE

**DOTTORATO DI RICERCA IN : SCIENZE DELLA TERRA
CICLO XXIII**

NON INVASIVE HYDROGEOLOGICAL TECHNIQUES FOR VADOSE ZONE HYDROLOGICAL CHARACTERIZATION

Direttore della Scuola di Dottorato : Ch.mo Prof. GILBERTO ARTIOLI

Coordinatore : Ch.mo Prof. GIORGIO CASSIANI

Dottorando : MATTEO ROSSI

INDEX

ABSTRACT	1
1. INTRODUCTION	3
1.1 HYDROGEOPHYSICS IN HYDROLOGICAL SYSTEMS	8
1.1.1 The saturated zone	8
1.1.2 The vadose zone	9
1.2 GENERAL HYDROGEOPHYSICAL APPROACHES	10
1.3 APPLIED METHODOLOGY	16
2. PART I:	18
STEADY STATE HYDROLOGICAL PARAMETERS ESTIMATION	
“STOCHASTIC ANALYSIS OF CROSS-HOLE GPR DATA FOR SUBSURFACE CHARACTERIZATION”	
2.1 INTRODUCTION	18
2.2 METHODOLOGY	20
2.3 ANALYSIS AND DISCUSSION	25
2.3.1 Synthetic dataset	25
2.3.2 Hatfiled field site	30
2.3.3 Gorgonzola field site	34
2.4 CONCLUSIONS	39
3. PART II:	41
HYDROGEOPHYSICAL INVERSION VIA TRACER TEST MONITORING	
“VADOSE ZONE ‘PUSH DOWN’ EFFECT DETECTED VIA PARTICLE TRACKING ANALYSIS”	
3.1 INTRODUCTION	41

3.2 SITE DESCRIPTION	44
3.3 MONITORING TRACER INJECTION TEST	45
3.4 HYDROLOGICAL MODELS	46
3.4.1 Initial steady water flow state	46
3.4.2 Selection of the hydraulic parameters	49
3.4.3 Tracer injection simulations	56
3.5 HYDROGEOPHYSICAL MONITORING	57
3.6 PARTICLE TRACKING ANALYSIS	62
3.7 RESULTS AND DISCUSSION	63
3.8 CONCLUSIONS	64
4. CONCLUSIONS	66
REFERENCES	67

ABSTRACT

Hydrogeophysics is a discipline that emerged and had a great development in the last two decades. The aim of this discipline is the subsurface hydrological and hydrogeological characterization via non-invasive geophysical techniques. Conventional sampling techniques, for characterizing or monitoring the shallow subsurface, are typically sparsely distributed or acquired at an inappropriate scale. Non-invasive geophysical datasets can provide more dense 2D/3D information. The present work focused on the hydrological characterization of the vadose zone, as it is a challenging issue that may be more deeply and extended understood.

The dependence of the geophysical response on changes in soil moisture content, e.g. via changes in electrical resistivity or dielectric properties, is the key mechanism that permits the use of non-invasive techniques to monitor the vadose zone in time-lapse mode, i.e. via repeated measurements over time. The use of these techniques in different configurations in the shallow and deep vadose zones can provide high-resolution images of hydrogeological structures and a detailed assessment of dynamic processes in the subsurface environment. The data from non-invasive techniques can subsequently be used to calibrate physical-mathematical models of water flow in the unsaturated zone. The understanding of fluid-dynamics is the key to all hydrologically-controlled environmental problems. The hydrogeophysical approach is based on links that can be established between geophysical quantities and hydrological variables, such as water content and solute concentration, generally in the form of empirical or semi-empirical petrophysical relationships.

The classical hydrogeophysical approach in hydraulic parameters evaluation starts from the measured geophysical data to estimate the hydrological state, albeit careful is need at this step: essential is the knowledge achievable from field data and the relative accuracy in the physical translation. Anyway this is the starting point for the hydrological simulation. Subsequently the hydrological modelled parameters may be compared and evaluated with the hydrological quantities obtained from geophysics through the petrophysical relationships. This approach can lead to erroneous parameter inference, if the spatial resolution of the geophysical techniques is not taking into account.

A different approach can be proceed, to overcome this issue. In spite of translating geophysical parameters in hydrological quantities, the comparison may be done directly on the not-inverted geophysical data. The geophysical surveys can be simulated with a forward model, starting from the hydrological modelled properties distribution and applying the petrophysical relationship to reconstruct the geophysical spatially-distributed parameters. At this point geophysical measured and simulated data can be compared, with the aim of calibrate and validate the hydrological model

under examination. This second approach, not requiring geophysical inversions, is able to overcome artefacts deriving from the inversion procedure; but the resolution of the surveys must be considered, because an hydrological state should not be reproduced from geophysical methodologies, even if the two datasets, both simulated and measured, are in a perfect fitting.

The work is divided in two complementary parts. **The first part** is centred on the hydrological quasi-steady state characterization from cross-hole radar measurements. In many studies cross-borehole zero offset profiles (ZOP) are used to infer subsoil moisture content, which are a key topic in hydrological modelling and consequently in hydraulic parameters estimation. The principal aim of this work is to have a more complete view of how boreholes GPR ZOP measurements are informative of the subsoil geometry and distribution of relative permittivity. This is essential in moisture content estimation, uncertainty quantification and in the initial setting of parameters necessary for starting an hydrological model. For this purpose three different ZOP datasets are analysed: a synthetic dataset and two field-measured datasets.

The second part of the work is the hydrogeophysical inversion of a tracer test in the vadose zone, conducted at the Hatfield site (near Doncaster, UK). The path of a tracer in vadose zone may be masked from the variations of the physical status surrounding the dispersive plume; this could lead to erroneous interpretations of the evolving plume. The load of the new water, that moves under gravitational forces, produces the raising of the degree of saturation in the media just below the plume. This incidental effect could significantly contribute to geophysical signals and hydrological characterizations. The aim of this study is the recognition and distinction of the paths of the new injected fluid from the groundwater, already present in the system and activated from pressure variations, in a sort of “piston” effect. The discrimination between the new percolating water and the old pushed-down water is a key issue in aquifer vulnerability and soil pollution migrations, which can affect the vadose zone. In this second part the hydrogeophysical inversion is conducted: the simulated hydrological quantities are used to obtain a geophysical forward model of ZOP surveys, that should be compared with measured ZOP soundings. An estimation of the goodness of the hydrological model is then possible. A particle tracking code is then run to detect the exact evolution of the tracer plume in the subsurface. A comparison with the results from the inverted geophysical datasets is able to discriminate the tracer fluid from the old water of the system and to individuate where the geophysical imaging could be deceptive and misleading.

The present work is an example of the hydrogeophysical inversion methods, where great emphasis is focused on the characterization of the hydraulic state preceding the tracer injection test. Anyway the system must be stressed under artificial hydraulic states to force the parameters estimation and to limit the range of probable hydrological models.

1. INTRODUCTION

The field “hydrogeophysics” emerged in the 1990a as a multi-disciplinary subject that focuses on the use of geophysical methods for characterising subsurface features, determining hydrogeological properties and monitoring processes relevant to soil and groundwater processes. Hydrogeophysical methods can allow large scale aquifer characterisation, previously unobtainable through conventional hydrogeological techniques. In addition, time-lapse deployment of appropriate methods can give useful insight into complex subsurface processes, aiding hydrological model development and the assessment of groundwater restoration strategies.

Hydrology has traditionally relied upon the availability of point measurements: precipitation at rain gauges, stream discharge at stream gauges, groundwater potentiometric surface at boreholes and, more recently, soil moisture content as measured, for example, by time-domain reflectometry (TDR – Topp et al., 1982). This body of information is necessary, but often far from being complete. In particular, it has been largely demonstrated (e.g. Beven and Binley, 1992) that, given the point information above, there will always be a number of different models that reproduce equally well the observed hydrological data (such as river discharge). This equifinal nature of different models is limited to their capability of matching the observed limited and local data, and may not be reflected in their prediction capability, i.e. the model forecasts may differ substantially should the forcing conditions (e.g. precipitation) be changed beyond the observed values. This critical model limitation is essentially driven by the fact that the actual structure of the subsurface is poorly known in terms of geometry, geology and hydraulic properties; this limitation often forces the models to be black boxes, either explicitly or implicitly due to the poor knowledge of the actual system characteristics.

Overcoming these serious limitations of hydrological modelling is not related to the nature of the models, but rather requires extra information. This is one of the fundamental needs addressed by hydrogeophysical measurements.

Hydrology research has developed a number of sophisticated tools to try and account for model uncertainty, particularly with respect to the limited knowledge of the subsurface in terms of its hydraulic property distribution. This is the reason for the focus in the present work on simply, but well developed and tested hydrological models; we are convinced that more interest must be centred on the information achievable from subsoil, especially in terms of widespread hydrological properties distributions. To overcome this lack, heavy reliance was initially put on densely monitored sites with hundreds of boreholes drilled over few hectares (e.g. LeBlanc et al., 1991), but this approach could not be realised except at a few advanced research sites. As a consequence, during the 1990s there was a rapid growth in the use of geophysics to try and provide spatially dense quantitative information about hydrological properties and processes. This need, in addition to the growing availability of fast field acquisition instruments and powerful computational tools, has led to much of the current developments in hydrogeophysics.

In addition to the above, important new requirements have been posed lately upon hydrological characterization and modelling: in particular, the growing issue of water quality requires that the presence and location of contaminants be assessed, and their migration in the hydrological system be monitored. The limitations of hydrological modelling and point measurements are even more severe in the case of water quality than in water quantity assessment. Here too geophysical methods have a potential role.

In summary, hydrogeophysics is asked to provide data for these three central purposes: subsurface structural characterization, fluid-dynamics description, and the recognition of presence and motion of contaminants.

Geophysics has long been used to support hydrogeological studies, but mainly for lithological boundary delineation (e.g. Giustiniani et al., 2008), i.e. to support structural and geometrical characterization of aquifers. This use of geophysics does not fully exploit the geophysical

measurements, but rather seeks to highlight contrasts in whatever physical property can distinguish one geological formation from its neighbours. This classical approach is anyway of basic interest in those subsurface system that are not well known, the essential first step before exploring and relating physical quantities estimated from geophysical soundings. In fact, geophysics has long been used also to exploit the physical nature of measurements, and translating these measurements into quantitative estimates of the soil/rock properties of interest. This translation requires that suitable constitutive laws link physical and structural properties of soil/rock, and the relevant discipline is petrophysics (e.g. Mavko et al., 2009).

In view of the needs above, the current developments in hydrogeophysics are aimed at providing quantitative information on the hydrological and hydraulic characteristics of the soil and subsoil, as well as quantitative data on the presence and motion of fluids and solutes in and out of the subsurface. Hydrogeophysics is therefore becoming a key instrument towards an effective characterisation of hydrological systems.

Among the available geophysical methods, not all of them are equally suitable for hydrogeophysical applications. Each geophysical technique measures at least one physical quantity:

- SEISMICS: elastic moduli and density
- GRAVIMETRY: density
- MAGNETICS: susceptibility and permanent magnetization
- GEOELECTRICS (DC resistivity, e.g. electrical resistivity tomography (ERT)): electrical conductivity
- GEOELECTRICS (induced polarization (IP)): complex electrical conductivity
- ELECTROMAGNETIC METHODS (EM): electrical conductivity

- SELF POTENTIAL (SP): electrical conductivity and potential sources
- GROUND PENETRATING RADAR (GPR): dielectric constant, electrical conductivity
- NUCLEAR MAGNETIC RESONANCE (NMR): number or protons, free pathway in pores, electrical conductivity.

In view of the hydrological aspects described above, potentially all geophysical methods can have some useful hydrogeophysical application, particularly in terms of structure characterization. However, some techniques have a more specific link to hydrological properties and to the presence/motion of water: these are underlined above. In particular the physical quantities more specifically affected by water presence or motion are, among the ones most commonly measured, electrical conductivity via ERT (Binley and Kemna, 2005) and dielectric constant via GPR (Annan, 2005). Other more specialized measurements (IP, SP and NMR) have strong connection to the pore-medium structure and presence/motion of water, solutes and free-phase contaminants, but are still of less common use as the relevant signal can be either below ambient noise or of uncertain attribution to hydrological causes.

In this work the focus is centred on ERT and GPR techniques, since these measurements are highly informative of the subsurface status, fast acquiring in boreholes arrays and the signals are clear linked to hydrological properties, especially in time-lapse monitoring.

	Structure	Fluid dynamics	Contamination
Gravimetry	+	++	
Magnetics	+		
Seismics	++	+	
DC resistivity	++	++	+
Electromagnetics	+	++	+
Induced Polarization		++	++
Self Potential	+	+	+
GPR	+	++	+
NMR	+	++	

Table 1: Use and effectiveness of geophysical methods for hydrological studies.

1.1 HYDROGEOPHYSICS IN HYDROLOGICAL SYSTEMS

Hydrological studies are always subdivided in two large categories, depending on the environmental compartments of interest: saturated zone or vadose (unsaturated) zone. These compartments are not really separated in nature, belonging to the same underground system, but they present high differences. They diverge not only in terms of their hydrological role and mechanisms, but also in terms of the hydrogeophysical measurements that can be conducted profitably on them.

1.1.1 The saturated zone

On time, the focus on saturated zone has been progressively shifting from water quantity to water quality problems. Transport of dissolved substances in groundwater is the most important mechanism controlling the migration of pollutants in the subsurface and is strongly controlled by geological heterogeneity at a variety of scales. In particular, hydraulic conductivity can vary by up to thirteen orders of magnitude. This fact has as a consequence a strong spatio-temporal variability of solute concentrations, that makes conventional monitoring techniques, based on few boreholes and limited water sampling in space and time, often incapable of capturing the variability of transport properties, as well as the complexity of transport processes. Hydrogeophysics can provide spatially and temporally dense information on the evolution of solute plumes, particularly during tracer tests (Kemna et al., 2002; Kemna et al., 2006; Cassiani et al., 2006a; Monego et al., 2010). The geophysical time-lapse data are used as equivalent concentration data to infer the timing and location of tracer breakthrough. In conjunction with transport models, such data can be directly interpreted in terms of transport parameters, such as flow velocity and dispersivity (Slater et al., 2002; Kemna et al., 2002; Singha and Moysey, 2006; Singha and Gorelick, 2006a,b; Day-Lewis and Singha, 2008).

1.1.2 The vadose zone

While the saturated zone has the long-established attention of aquifer studies, a traditional area of interest of subsurface hydrology, the vadose zone usually is poorly studied and understood. It's due to the difficulties of achieving knowledge with the classical hydrological methods, that most in this case can provide few sparsely point data, not sufficient for a widespread and detailed properties distribution. The present work focused exactly on the hydrological characterization of the vadose zone, as it is a challenging issue that may be more deeply and extended understood.

The vadose zone, i.e. the part of subsurface above the water table, is home to a number of key processes that control the mass and energy exchanges between the subsurface and soil surface. Vadose zone hydrology provides information about exchanges with the soil compartment, and from there with the atmosphere, and subsurface water migration, with strong implications in water resources management: aquifer recharge is controlled by movement through the vadose zone. Contaminants released from the surface invade the vadose zone and, before reaching the aquifer system underneath, can be altered, retarded or wholly removed by biological, chemical and physical processes in the vadose zone. Unsaturated processes control also the availability of water for agriculture, and are the driving mechanisms in slope stability, floods and other major engineering geology problems.

As mentioned previously, the hydrology of the vadose zone is poorly known, mainly because of technical limitations in sampling and access just at one or two metres below ground. The most useful measurements of unsaturated zone conditions (moisture content via TDR and suction via tensiometers) are limited to no more than a couple of metres depth. Extensive monitoring over large areas is labour intensive and time consuming, and they are essentially local scale measurements.

The vadose zone deeper than a couple of metres below ground surface can be mapped from the surface, at the expense of severe resolution losses, and more efficiently using borehole geophysical

methods: single-borehole, borehole-to-borehole and borehole-to-surface geophysical measurements achieve a resolution sufficient for quantitative hydrologic interpretation (Slater et al., 1997b; Binley et al., 2001, 2002a,b; Binley and Beven, 2003; Cassiani et al., 2004; Cassiani and Binley 2005, Chang et al., 2006, Deiana et al., 2007, 2008, Looms et al., 2008a,b; Koestel et al., 2008; Cassiani et al., 2008 ,2009b; Cassiani et al., 2006a). In most cases the ultimate goal is the identification of hydraulic properties and parameters of the vadose zone. The dependence of the geophysical response on changes in soil moisture content, e.g. via changes in electrical resistivity or dielectric properties, is the key mechanism that permits the use of non-invasive techniques to monitor the vadose zone in time-lapse mode, i.e. via repeated measurements over time. The use of these techniques in different configurations in the shallow and deep vadose zones can provide high-resolution images of hydrogeological structures and, in some cases, a detailed assessment of dynamic processes in the subsurface environment. Both natural infiltration processes and specifically designed tracer tests can be monitored over periods of time that can last from a few hours to several years. The data from non-invasive techniques can subsequently be used to calibrate physical-mathematical models of water flow in the unsaturated zone.

1.2 GENERAL HYDROGEOPHYSICAL APPROACHES

The understanding of fluid-dynamics is the key to all hydrologically-controlled environmental problems. The hydrogeophysical approach is based on links that can be established between geophysical quantities and hydrological variables, such as water content and solute concentration, generally in the form of empirical or semi-empirical relationships. Consider e.g. the classical relationships proposed by Archie (1942) for electrical conductivity and by Topp et al. (1980) and Roth et al. (1990) for the dielectric constant. Using such relationships, it is possible, albeit not always straightforward, to obtain quantitative estimates of hydrologic data.

These constitutive relationships are the base of the hydrogeophysical inversion, since the estimated hydrological quantities may be used in hydrological model calibration. In this manner hydrogeophysics is able to calibrate and validate models that may infer more knowledge on fluid dynamics and on the identification of the parameters of interest. The scheme in Fig. 1.1 summarizes the classical hydrogeophysical approach in hydraulic parameters evaluation. Measured geophysical data estimate the hydrological state, albeit careful is need at this step: essential is the knowledge achievable from field data and the relative accuracy in the physical translation. Anyway this is the starting point for the hydrological simulation. Subsequently the hydrological modelled parameters may be compared and evaluated with the hydrological quantities obtained from geophysics through the petrophysical relationships. This approach can lead to erroneous parameter inference, if the spatial resolution of the geophysical techniques is not taking into account. There are in fact portions of the subsurface exploration that are less covered from the soundings, and it depends on the specific geophysical methodology and on the adopted survey configuration.

A different approach can be proceed, to overcome this issue (Fig. 1.2). In spite of translating geophysical parameters in hydrological quantities, the comparison may be done directly on the not-inverted geophysical data. The geophysical surveys can be simulated with a forward model, starting from the hydrological modelled properties distribution and applying the petrophysical relationship to reconstruct the geophysical spatially-distributed parameters. At this point geophysical measured and simulated data can be compared, with the aim of calibrate and validate the hydrological model under examination. This second approach, not requiring geophysical inversions, is able to overcome artefacts deriving from the inversion procedure; but the resolution of the surveys must be considered, because an hydrological state should not be reproduced from geophysical methodologies, even if the two datasets, both simulated and measured, are in a perfect fitting.

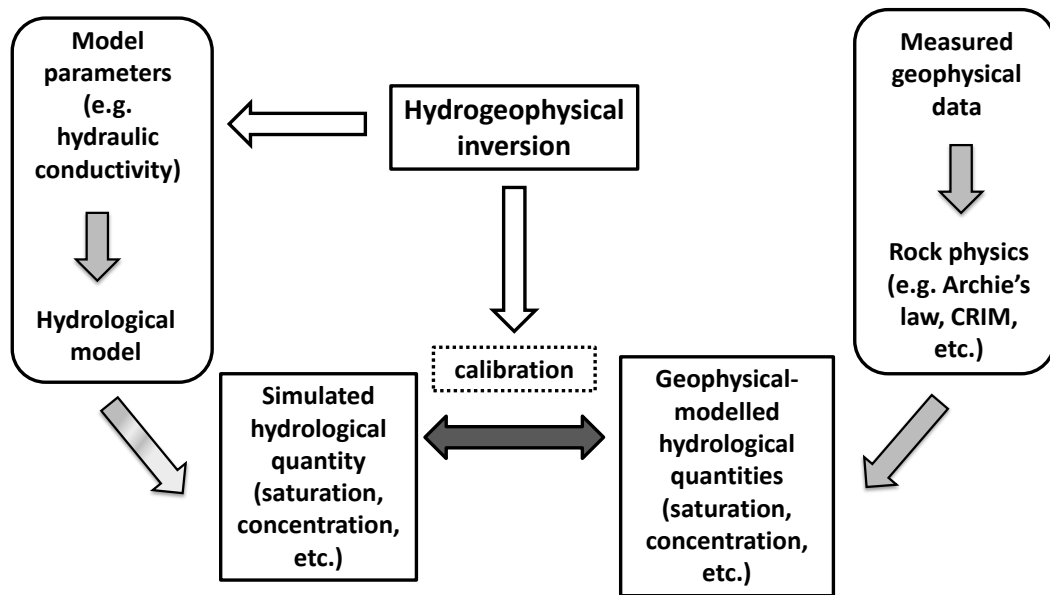


Fig. 1_ General scheme of classical hydrogeophysical inversion based on calibration of hydrological models on estimated hydrological quantities derived from geophysical data.

Intuitively, the calibration of hydrological model requires that the system is adequately stressed so that different states of the variables are explored. This condition is not guaranteed to be met under natural conditions. Consequently, it is faster and more informative to conduct controlled experiments that can be monitored in a time span of hours, days, or weeks depending on the dynamics of the system. Key to the possibility of using this approach is the capability of measuring geophysical quantities repeatedly over time. It is interesting to note that although numerous synthetic model studies have been utilised to demonstrate quantification of hydraulic properties from time-lapse geophysical studies, very few (e.g. Binley *et al.*, 2002a) have illustrated the approach in field-based studies.

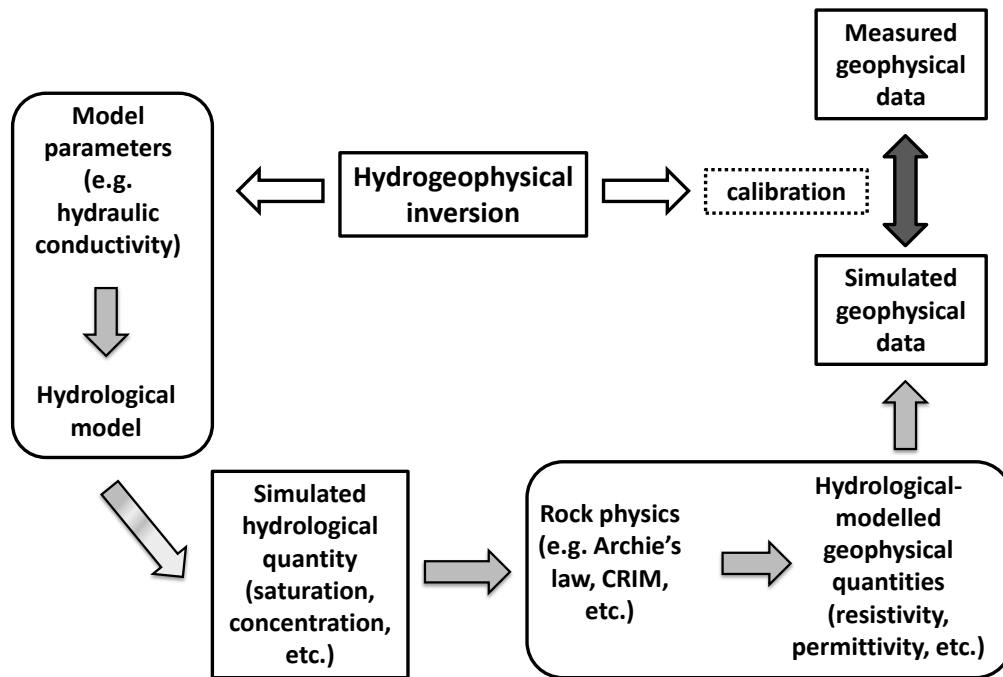


Fig. 1.2 _ General scheme of alternative hydrogeophysical inversion based on calibration of hydrological models on calculated geophysical data derived from hydrological quantities.

Today many shallow geophysical techniques have the potential to highlight two concurring aspects of the subsurface:

- (a) its **static** aspects, i.e. the characteristics that *do not* change over time, principally the geology;
- (b) its **dynamic** aspects, i.e. the characteristics that *do* change over time, and that are inherently linked to the motion of fluids, water above all.

If time-lapse measurements are made, changes in geophysical response at the same spatial location are generally linked to hydrological changes, e.g. in the vadose zone to changes in water saturation. Features that are not changing over time can be reasonably attributed to geological control: e.g. water saturation may be consistently different at different spatial locations as a consequence of lithological differences . This use of geophysical data requires:

1. that the collected geophysical data have a clear, identifiable and possibly quantitative meaning in terms of environmental variables of interest, e.g. water saturation;
2. that the resolution and sensitivity of geophysical methods in space and time is fully understood, in order to assess the actual information content in the data, and prevent, e.g., the erroneous interpretation of artefacts;
3. that hydrologic modelling be devised to be able to incorporate the non-invasive data in the most profitable and effective way, accounting for resolution, sensitivity and scale effects.

The three points above are, as of today, only partly achieved, and the actual work wants to examine at least part of these challenging issues .

The potential of hydrogeophysics faces also a number of limitations; challenges for the future are to overcome or at least circumvent some of these limitations. The most notable once are:

1. Geophysical data are limited in terms of resolution. This is true even in cross-hole configuration (Cassiani et al., 1998; Day-Lewis and Lane, 2004; Day-Lewis et al., 2005). The key consequence of this is that not the entire geophysical “image” has the same degree of accuracy and practically all inversion methods require some sort of a-priori information (e.g. smoothness) to ensure convergence. Interpreting (also, quantitatively) these hydrogeophysical images with no account for resolution limitations can lead to serious problems. The most notable one is the mass balance errors very often present in tracer tests monitored e.g. via ERT both in the saturated and the unsaturated zones (Binley et al., 2002a; Singha and Gorelick, 2005; Deiana et al., 2007, 2008).
2. Scale issues: most hydrogeophysical work has been conducted to date at the small scale. But hydrology needs large scale evaluation. For this reason some techniques that hold the promise to

develop into large scale time-lapse monitoring tools should be considered as top priority research areas.

3. Inversion and joint inversion is still computationally very expensive, especially in 3D and time-lapse. This, together with the acquisition time in the field, still limits out capability of fully exploiting the conceptual potential of hydrogeophysics.

4. There is a need to demonstrate the information content obtained from geophysical methods in hydrogeophysical studies. Much of the literature, to date, has focussed on developing and testing methods and approaches. For some problems, geophysics may not be an appropriate tool and there is a danger of overestimation (or assumed knowledge) of the information available from geophysics in some cases. Objective approaches are, therefore, needed in order to test the value of geophysics in hydrological investigations.

In summary, a number of key issues shall be considered when approaching hydrogeophysics as a hydrological tool:

1. The hydrologic behaviour of the shallow subsurface can be pictured via non invasive methods.
2. The information is maximized by time-lapse measurements and strong changes.
3. Constitutive laws linking hydrology and geophysics are essential.
4. The acquisition and inversion characteristics of the adopted hydro-geophysical methods have critical impact (e.g., scale effect).
5. The importance of auxiliary information concerning lithology and geology cannot be overstressed.

1.3 APPLIED METHODOLOGY

The present work is focused on the application of the hydrogeophysical method on field measurements, regarding the vadose zone. Geophysical data are collected at different sites, where boreholes are installed for ERT and GPR soundings.

The work is divided in two complementary parts. **The first part** is centred on the hydrological quasi-steady state characterization from cross-hole radar measurements. In many studies cross-borehole zero offset profiles (ZOP) are used to infer subsoil moisture content, which are a key topic in hydrological modelling and consequently in hydraulic parameters estimation. The principal aim of this work is to have a more complete view of how boreholes GPR ZOP measurements are informative of the subsoil geometry and distribution of relative permittivity. This is essential in moisture content estimation, uncertainty quantification and in the initial setting of parameters necessary for starting an hydrological model. For this purpose three different ZOP datasets are analysed: a synthetic dataset and two field-measured datasets.

The second part of the work is the hydrogeophysical inversion of a tracer test in the vadose zone, conducted at the Hatfield site (near Doncaster, UK). The path of a tracer in vadose zone may be masked from the variations of the physical status surrounding the dispersive plume; this could lead to erroneous interpretations of the evolving plume. The load of the new water, that moves under gravitational forces, produces the raising of the degree of saturation in the media just below the plume. This incidental effect could significantly contribute to geophysical signals and hydrological characterizations. The aim of this study is the recognition and distinction of the paths of the new injected fluid from the groundwater, already present in the system and activated from pressure variations, in a sort of “piston” effect. The discrimination between the new percolating water and the old pushed-down water is a key issue in aquifer vulnerability and soil pollution

migrations, which can affect the vadose zone. In this second part the hydrogeophysical inversion is conducted as summarized in the scheme of Fig. 1.2: the simulated hydrological quantities are used to obtain a geophysical forward model of ZOP surveys, that should be compared with measured ZOP soundings. An estimation of the goodness of the hydrological model is then possible.

A particle tracking code is then run to detect the exact evolution of the tracer plume in the subsurface. A comparison with the results from the inverted geophysical datasets is able to discriminate the tracer fluid from the old water of the system and to individuate where the geophysical imaging could be deceptive and misleading.

2. PART I: STEADY STATE HYDROLOGICAL PARAMETERS ESTIMATION

“STOCHASTIC ANALYSIS OF CROSS-HOLE GPR DATA FOR SUBSURFACE CHARACTERIZATION”

M. Rossi ¹, G. Cassiani¹, A. Binley², R. Deiana¹

¹ Dipartimento di Geoscienze - Università degli Studi di Padova

² Lancaster Environmental Centre - Lancaster University

2.1 INTRODUCTION

Ground penetrating radar (GPR) is a well-established geophysical technique, that has been applied for about two decades. In particular GPR is used, via specific relationships, to estimate hydrological parameters in vadose zone, i.e. moisture content, both from the surface and in boreholes (e.g. Cassiani et al., 2006; Kemna et al, 2002; Binley et al., 2002).

The velocity of electromagnetic waves in a medium, v , is related to the bulk relative dielectric permittivity (or bulk dielectric constant), ϵ_r [-], of the medium itself:

$$v = \frac{c}{\sqrt{\epsilon_r}} \quad (2.1)$$

where c is the radar wave velocity in air (≈ 0.3 m/ns). There are relationships that link ϵ_r to volumetric moisture content (θ), as the empirical Topp equation (Topp et al. 1980)

$$(2.2)$$

or the semi-empirical complex refractive index method (CRIM) (Roth et al., 1990)

$$\epsilon_r = \epsilon_{gr} + \epsilon_w + \epsilon_a + \epsilon_p \quad (2.3)$$

where ϵ_{gr} is the permittivity of the sediment grains, ϵ_w is the permittivity of water, ϵ_a is the permittivity of air and ϵ_p is porosity.

In many studies cross-borehole zero offset profiles (ZOP) are used to infer subsoil moisture content, which are a key topic in hydrological modelling and consequently in hydraulic parameters estimation (e.g. Deiana et al., 2008; Looms et al., 2008; Cassiani et al., 2004). ZOP borehole measurements are very useful to detect subsoil dielectric properties, due to their simplicity in data collection, treatment and analysis.

Different approaches were developed to obtain hydraulic parameters from ZOP surveys. The easiest is the direct-wave approach, where point ZOP travel times are converted into velocity and subsequently to ϵ_r estimates using eq. 2.1. This approach could be misleading as it does not take into account two essential factors: volume averaging (Fresnel zone) and critical wave refractions, that can occur between sharp ϵ_r boundary transitions.

Cassiani and Binley (2005) analysed the crosshole radar response over a long time series. The 50 MHz radar-derived moisture content profiles were obtained taking into account the vertical scale of measurements, with an averaging window size of the order of the antenna length and the Fresnel zone width. The authors performed a stochastic inversion (Monte Carlo approach), averaging the simulated moisture content profile on a moving window of 2 m and comparing it with the moisture content profile inferred from the measured ZOP. The best simulation that matches the measured profile shows a geometry very different from the averaged profile. This result confirms that caution is needed in the interpretation of radar ZOPs.

Rucker and Ferré (2004) analysed the impact of critically refracted waves on a first arrival travel time profile, derived from ZOP measurements in a layered system with sharp changes in water content. The improvement, via an inversion with a refracted ray tracing method, is essential to correct the moisture content profile calculated from direct wave interpretation.

The principal aim of this work is to have a more complete view of how boreholes GPR ZOP measurements are informative of the subsoil geometry and distribution of relative permittivity. For this purpose an electromagnetic (EM) wave simulator has been applied within a stochastic Monte Carlo framework. In this manner both averaging and critically refracted wave effects are taken into account. Results from synthetic and real ZOP datasets are statistically analysed to deduce what kind of subsoil ϵ_r -distributions are resolvable and well defined with a degree of uncertainty.

2.2 METHODOLOGY

The approach adopted in this study has the aim of analysing borehole ZOP measurements to infer knowledge about the distribution and the relatively uncertainty of the achieved ϵ_r values. The simply direct-wave method is compared with the results obtained from a stochastic inversion. A Monte Carlo framework is carried out, generating several thousand possible system geometries, which are capable to explore the underground complexity of dielectric materials. The aim of the stochastic approach is to reconstruct what kind of dielectric properties distributions are capable to produce the signal measured with the ZOP sounding.

The inversion is performed running a Monte Carlo simulation of several tens of thousands realizations (Fig. 2.1). Every realization generates a random ϵ_r geometry, used as input for the EM wave propagation simulator GprMax2D software (Giannopoulos, 2005), from which the first arrival travel time profile is extracted, and subsequently statistically compared with the real measured ZOP

sounding. For the generation of ϵ_r distributions, the subsurface is idealized as horizontally layered, with anisotropy only on the vertical direction. This simplification is essential to limit the potential variability of spatial distributions. The mono-dimensional approximation is reasonable in sediment covers, because transmitting and receiving antennae are not so far (boreholes are usually less than 10 m apart), so the underground materials are not expected to vary significantly. Moreover ZOP soundings are not appropriate to detect lateral variabilities as the multiple offset gather, due to the restricted and embedded information of a borehole ZOP sounding and the lack of coverage of crossing ray paths.

The material properties generated are limited to dielectric permittivity, all media are considered as perfect conductance (electrical conductivities of 0 S/m) to avoid wave attenuation and individuate a more precise first arrival travel time.

In GprMax2D the physical structure of the GPR antenna is not included in the model, then the antenna is modelled as an ideal Hertz dipole. The 2D code is run instead of GprMax3D software, in spite of the real underground system is three dimensional. This choice is due to the more time consuming 3D code, not useful computing a Monte Carlo simulation. To validate the use of the 2D code, a comparison between 2D and 3D software is performed (Fig. 2.2). The 3D model has the same 2D layered subsoil system, but extended in the third direction.

Several synthetic ϵ_r -profiles are used as input for three cases: one 2D and two 3D models. Here only the results of one profile are shown, anyway the other tested profiles give similar outcomes. The first case is performed running GprMax2D, where the antennas are perpendicular to borehole directions. The second case with GprMax3D has the same orientation of antennas as the two-dimensional case. The third case is achieved running GprMax3D with the antenna dipole oriented vertically, exactly as in a borehole field experiment.

The results show a perfect match between the first-arrival travel times obtained from the three models, as it is clear in Fig. 2.2. Small differences are simply due to the picking of first arrival EM wave propagation. This result justifies the use of the 2D code in the stochastic analysis, computing lighter than the corresponding 3D code.

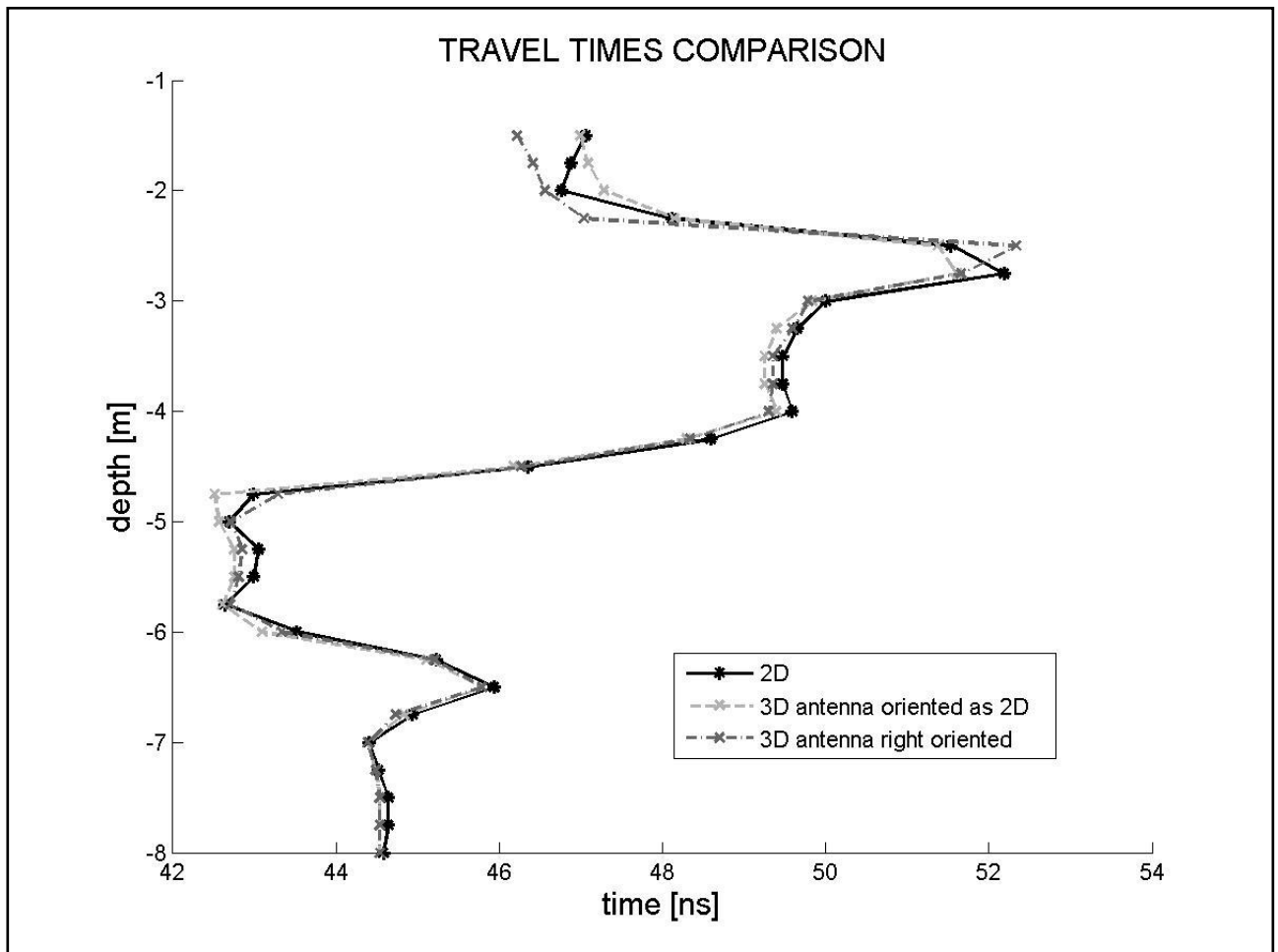


Fig. 2.2 – Comparison between results of 2D and 3D codes (with different antenna orientation).

From every single Monte Carlo realization, derived from a random relative permittivity profile, the calculated first-arrival travel times are extracted. Calculated and true travel times are compared and evaluated with the aim to obtain the unknown dielectric permittivity layering with an estimation of the goodness of fit and a subsequent uncertainty range.

Measured and simulated travel time profiles are not compared entirely, but each travel time is compared individually. This is done to increase the information suitable from the low number of realizations, due to very long computational times and the low probabilities to obtain travel time profiles that fit the measured data at every shot. In fact a generated travel time profile may reasonably match the field derived travel times in a reduced portion, but it could show an extremely poor fit on the other segments, especially in complex heterogeneous subsoil. Analysing every single travel time, the differential fitting between the profiles is overcome; nevertheless the contribute from surrounding media must be considered in every shot position, at least for a reasonable large Fresnel volume.

For every single ZOP shot, real (TT_r) and simulated travel times (TT_i) are statistically compared using chi-squared factor to estimate the goodness of fit:

$$- \tag{2.4}$$

where n are the degrees of freedom, in this case equal to 1, and σ is the measurement error standard deviation. The measurement error is unknown and it depends on many features: operators, environment, media properties; for this reason different values of standard deviation, realistic for the cases reported in this study (from 0.5 to 1.5 ns), are employed. Only values of less or equal to 1 are stored (reduced chi-squared factor):

$$(2.5)$$

The interest is focused on ε_r values related to all simulated travel times (TT_i) that satisfy equation (2.5). For these values, the Fresnel volume is calculated in a interactive method, starting with the velocity obtained directly from TT_r plus 50%. At each iteration the Fresnel volume is computed and the mean ε_r value inside it is achieved. Then the posterior velocity is deduced from

the mean ϵ_r value and compared with the prior velocity; this procedure goes on until the error between the two subsequent velocities is less than 5%.

In the end, the magnitude of the vertical segment around the position of each transmitter-receiver depth is obtained, i.e. the Fresnel ellipsoid minor axis. The distribution of ϵ_r values, generated at that realization and related to each detected vertical segment, is stored. Where overlapping segments are present, ϵ_r -distributions are intersected to preserve only values present in both ϵ_r sets. This is useful to prevent erroneous data storage as consequence of the averaging ϵ_r values inside the Fresnel volume; this is essentially caused to an overestimation of the mean velocity and of the Fresnel ellipsoid minor axis at that precise shot. This procedure is applied to all travel times for every single realization and the results are merged to achieved, in conclusion, an overall permittivity distribution with depth, as it is shown in Fig. 2.3.

At this point, an uncertainty quantification of ϵ_r in function of depth is possible. Deriving median, mean and data variance, in some cases an estimation of permittivity geometry is feasible, while in other instances a large confidence range leads to the impossibility of layers definition.

2.3 ANALYSIS AND DISCUSSION

Three different datasets are analysed. First, a synthetic cross-hole GPR dataset is considered, where a first arrival travel times profile is obtained from a well known ϵ_r distribution. The other datasets are measured ZOPs collected from two field sites: Hatfield (UK) and Gorgonzola (Italy).

2.3.1 Synthetic dataset

A synthetic case is first analysed, since the results can be validated with the established permittivity geometry of the system. In real field cases the media distribution is unknown, being the focus of the geophysical inversion.

The synthetic case is an alternating sequence of fine, thin layers (highest ϵ_r values) and coarse, thick layers (lower ϵ_r values). Alternating lithological sequences are common in shallow sediment covers and they are hard to define from ZOP sounding, usually unable to recognise a complex system with changing material properties, as mineralogy and moisture content.

The synthetic profile, taken as the *true* field-measured ϵ_r profile, is a one-dimensional ϵ_r distribution with homogeneous values in each layer (Fig. 2.1 *syn* and Chi *syn*). To recognise the validity of the stochastic method, sharp or softer ϵ_r contrasts are introduced.

The EM simulator GprMax2D is then run to obtain the first arrival travel times profile from the *true* ϵ_r geometry (Fig. *allTT- ϵ_r syn*). Transmitter and receiver antennas of 100 MHz frequency are virtually placed in different boreholes, 5 m apart, and lowered simultaneously of 0.25 m from -1.5 to -8 m depth. The first shot is located at -1.5 m depth to avoid critically refracted waves in air, that kind of analysis is not in the purpose of this study.

The geometry of the system is made to vary in a Monte Carlo simulation, albeit with some well-defined constraints: ranges of thickness and approximate location of the layers; to maintain the alternating sequence, but exploring layers displacing and properties. Relative permittivity ranges are chosen according to the literature.

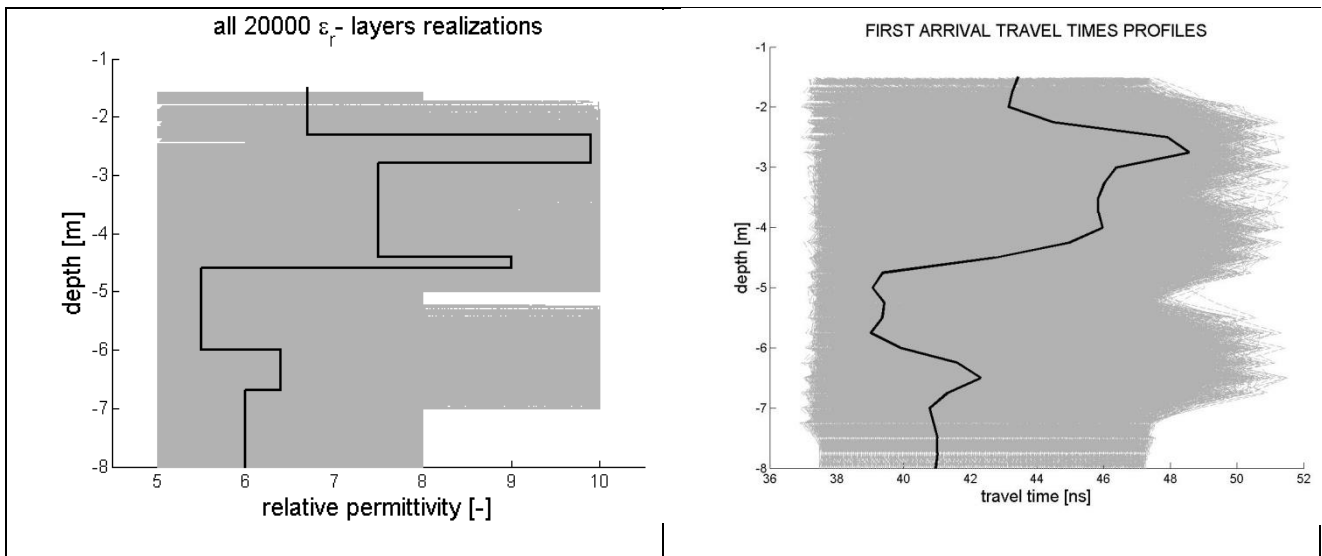


Fig. allTT- ϵ_r syn _ On the left, all the 20000 simulated ϵ_r profiles (grey dashed lines) and the real ϵ_r distribution (solid black line). On the right, all the 20000 travel times profiles (gray dashed lines) and the real travel time profile (solid black line). CAMBIA QUESTE IMMAGINI????

The methodology described in the previous 2.2 section is applied in a Monte Carlo simulation with 20000 realizations (Fig. 2.2). Fig. 2.3 shows the resulting ϵ_r distributions as a function of depth with four different standard deviation values ($\Delta = 0.75, 1.0, 1.25, 1.5$ ns), applied in the reduced chi squared analysis, which are related to different grades of probable measurement errors. The *true* ϵ_r profile and the ϵ_r profile directly derived from first-arrival travel times is also plotted in Fig. 2.3.

As the error variance is changed, so change the goodness of fit. The broader ranges at the top and the bottom of the profile are due to poor constraints, derived from the lack of shots in those fractions and from the superimposition of few Fresnel volumes.

The red dashed lines in Fig. 2.3 reproduce the ϵ_r curve deduced directly from the *true* first-arrival travel times (eq. 2.1). A large discrepancy is present between the curve and the *true* ϵ_r profile (solid black line): the sharp geometry is smoothed and slower media are underestimated in ϵ_r . The finer high permittivity layer at about -2.6 m depth is not reproduced in its features and the ϵ_r value is underestimated. The narrow fine layer located at about -4.3 m is completely invisible for the direct-wave profile, in spite of its relevance in hydrogeological characterization.

The variance of ϵ_r , derived from the stochastic approach, is about centred around the real profile, meaning that the results are close to the real physics of the system. Fig. 2.4 shows statistical parameters for the four different error standard deviation assumptions in the reduced chi-squared factor analysis (eq. 2.4).

It is evident that the stochastic method defines the layers geometry with more accuracy and it is able to reproduce sharper boundaries than the direct-wave approach. A relevant aspect of this analysis is the clear vision of what can be solved from cross-hole radar measurement. Note that thin layers with high ϵ_r are not well defined, and the corresponding ranges are spread over broad permittivity values. This evidence is clear in Fig. 2.4 at depth of about -2.6, -4.3 and -6.5 m, where the 'true' ϵ_r values are underestimated from statistical analysis, due to the broad dispersion in these thin and slower layers. Anyway relevant improvements, respect the direct-wave method, are the individuation of a thin layer centred at -4.3 m and the higher mean permittivity values detected at -2.6 and -4.3 m. In fact the direct-wave approach is not able to reproduce the magnitude of real ϵ_r values. This aspect is the consequence of refraction phenomena: first arrivals are characterized from a path that involves faster and thicker layers.

The statistical analysis, consequently, demonstrate that in real cases thin clay layers, for example, could be invisible to investigation, underestimated or misinterpreted, in spite of their high relevance

in hydrological processes. Thicker layers have, on the contrary, narrow range boundaries, where permittivity could be determined with a good degree of uncertainty.

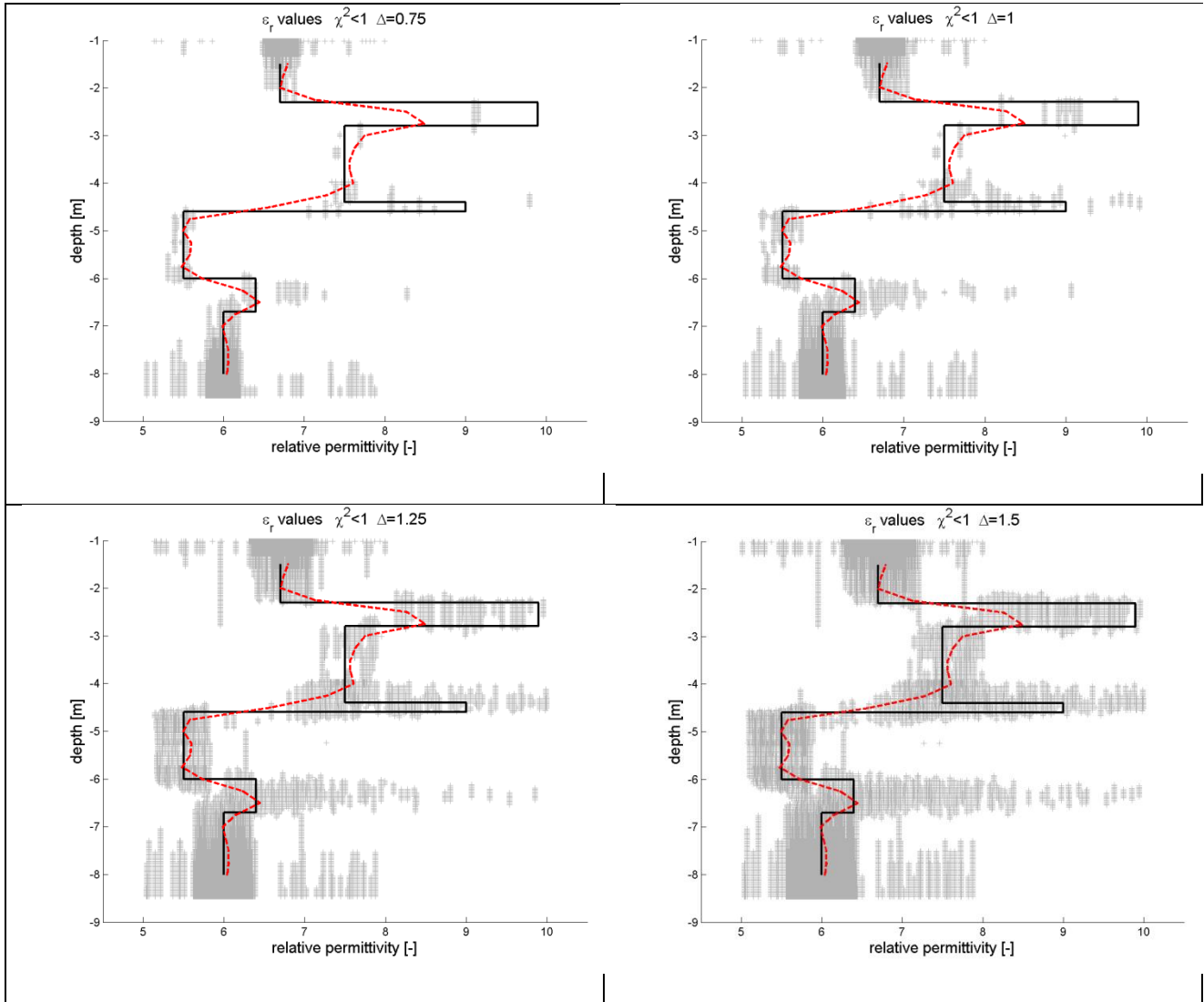


Fig. 2.3 _ Synthetic dataset. Distributions of ϵ_r values (light-grey crosses) after the reduced chi-squared analysis on 20000 realizations, with different standard deviation values (0.75, 1.0, 1.25, 1.5 ns) in the reduced chi-squared factor. Black line is the true 1-D ϵ_r profile and red dashed line is the ϵ_r profile obtained from the direct-wave approach.

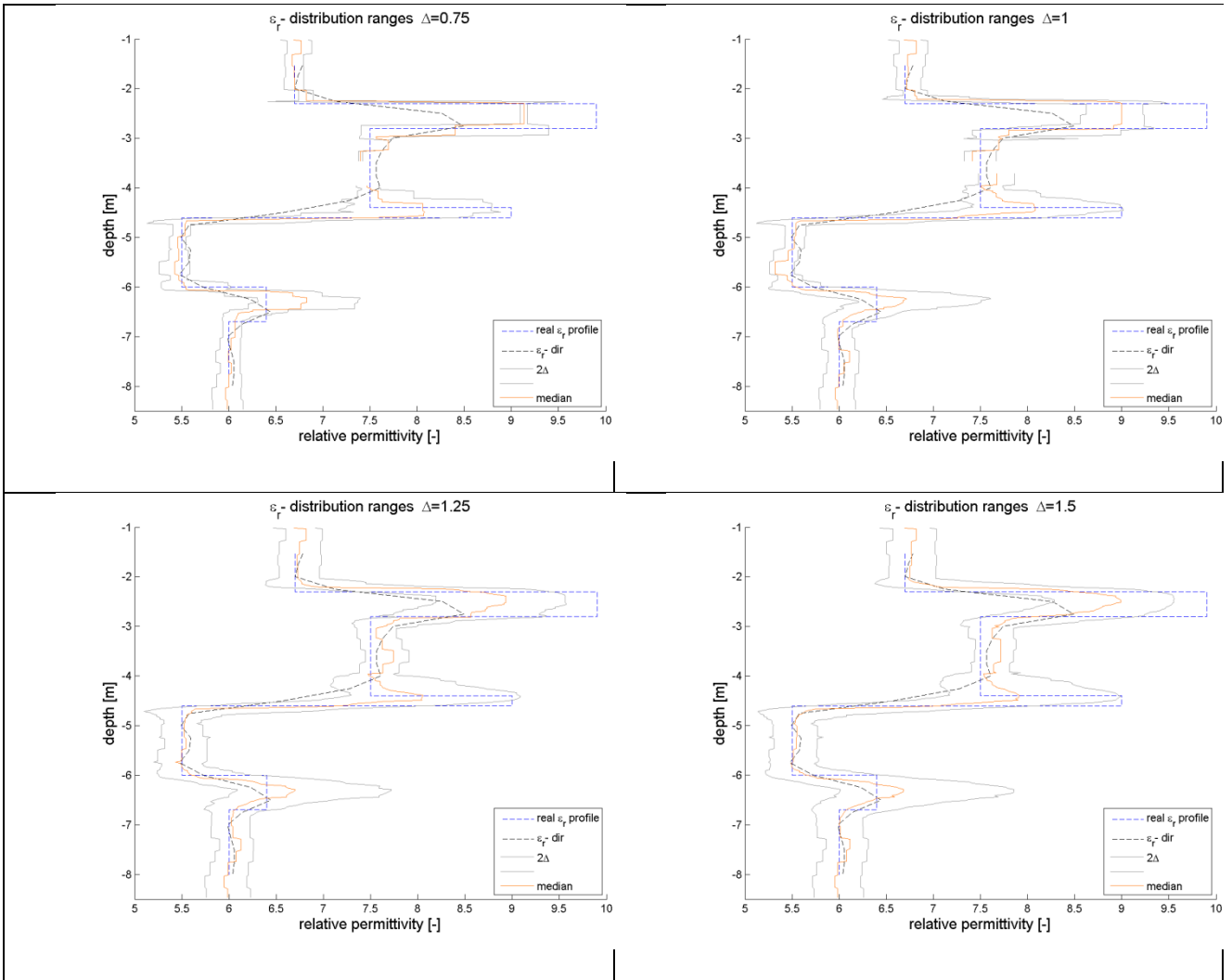


Fig. 2.4 _ Synthetic dataset: different error standard deviation values (0.75, 1.0, 1.25, 1.5 ns) in the reduced chi-squared factor. Grey lines are ϵ_r -range boundaries as function of depth, accounted as two times the data standard deviation around the mean value. Orange line is the median of the data distribution, blue dashed line is the 'true' ϵ_r profile and black dashed line is the ϵ_r -profile from the direct-wave approach.

2.3.2 Hatfiled field site

A field dataset is also considered. The field site is located at Lings Farm, Hatfield (near Doncaster, UK) on the outcrop of the Sherwood Sandstone. Binley et al. (2001) show lithological logs from two cores extracted from the site. The main lithology is medium-grained sandstone, interspersed with interlaminated fine and medium grained sandstones, particularly in the zone around -6 m depth, and between -8 and -9 m. Drift at the top of the section at the site is typically 2-3 m thick, and consists mainly of fluvio-glacial sands, derived from the underlying sandstones, with frequent large pebbles/cobbles. The cores were extracted about 20 m apart the radar boreholes, so a direct comparison with the results of the study is not possible, due to the lateral variability in positions and thicknesses of layers.

During March 2003 a ZOP sounding was performed (Winship et al., 2006) with a Sensors and Software Pulse EKKO PE100 system (Sensors & Software, Mississauga, ON, Canada) and 100 MHz antennas. The antennas were lowered at 0.25 m increments from -2 to -10 metres below the surface.

The same stochastic methodology for the synthetic dataset was applied. The geometry of the system was varied within a Monte Carlo simulation (20000 realizations), but constrained in a range of thickness and location of the layers, to maintain the alternating sequence of materials observed from drill cores taken at the site.

The results are show in Fig. 2.5. The ϵ_r distribution is set around the ϵ_r profile derived from direct-wave inversion (red dashed line), using experimental travel times. The representation of statistical parameters in Fig. 2.5 is helpful to individuate uncertainties in the profile. The poor definition of the fractions from -2.5 to -3.5 m and from -9 to -10 m is due to the high and sharp media contrast, not well resolvable with 20000 realizations and low error standard deviation values.

The abrupt change in material properties could not be well reconstructed with the direct-wave approach, which shows a smooth profile, while stochastic approach individuates sharper ϵ_r transitions, as is well described in the core logs. Sharp media boundaries are clear individuated at -2.8, -4.6 and -9 m depth. Three broader ϵ_r ranges are located around -2.5, -4.3 and -6.5 m depth. The larger uncertainty at these positions could be related to finer and thinner sediments, as found in the synthetic case.

This thin layers could be essential in an hydrological characterization for their low fluid conductivity and high residual moisture content, anyway they could not be defined with accuracy due to the higher uncertainties, that derived from refraction and averaging effects.

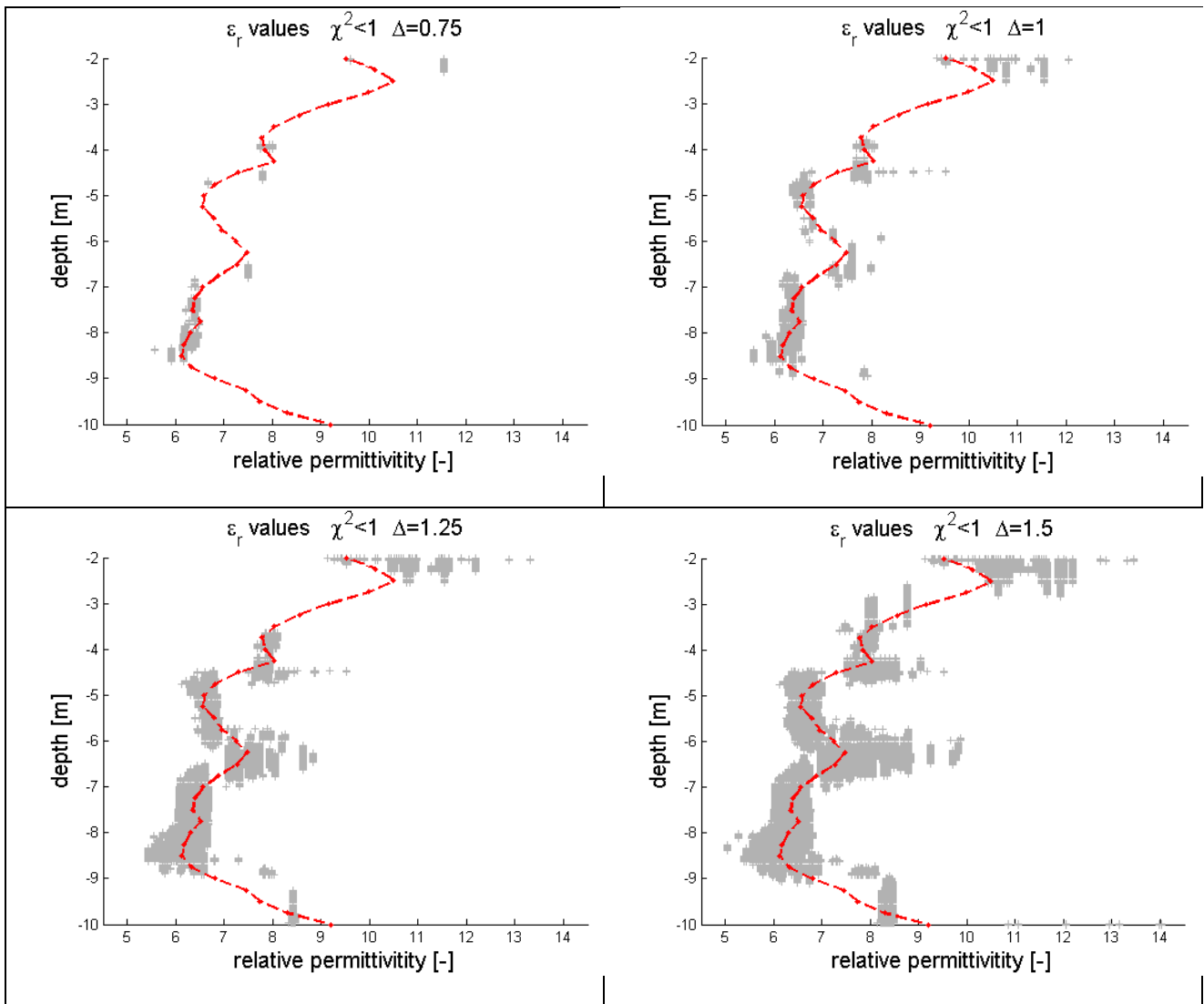


Fig. 2.5 – Hatfield site dataset. Distributions of ϵ_r values (light-grey crosses) after the reduced chi-squared analysis on 20000 realizations, with different standard deviation values (0.75, 1.0, 1.25, 1.5 ns). Red dashed line is the ϵ_r profile directly obtained from experimental first-arrival travel times (direct-wave approach).

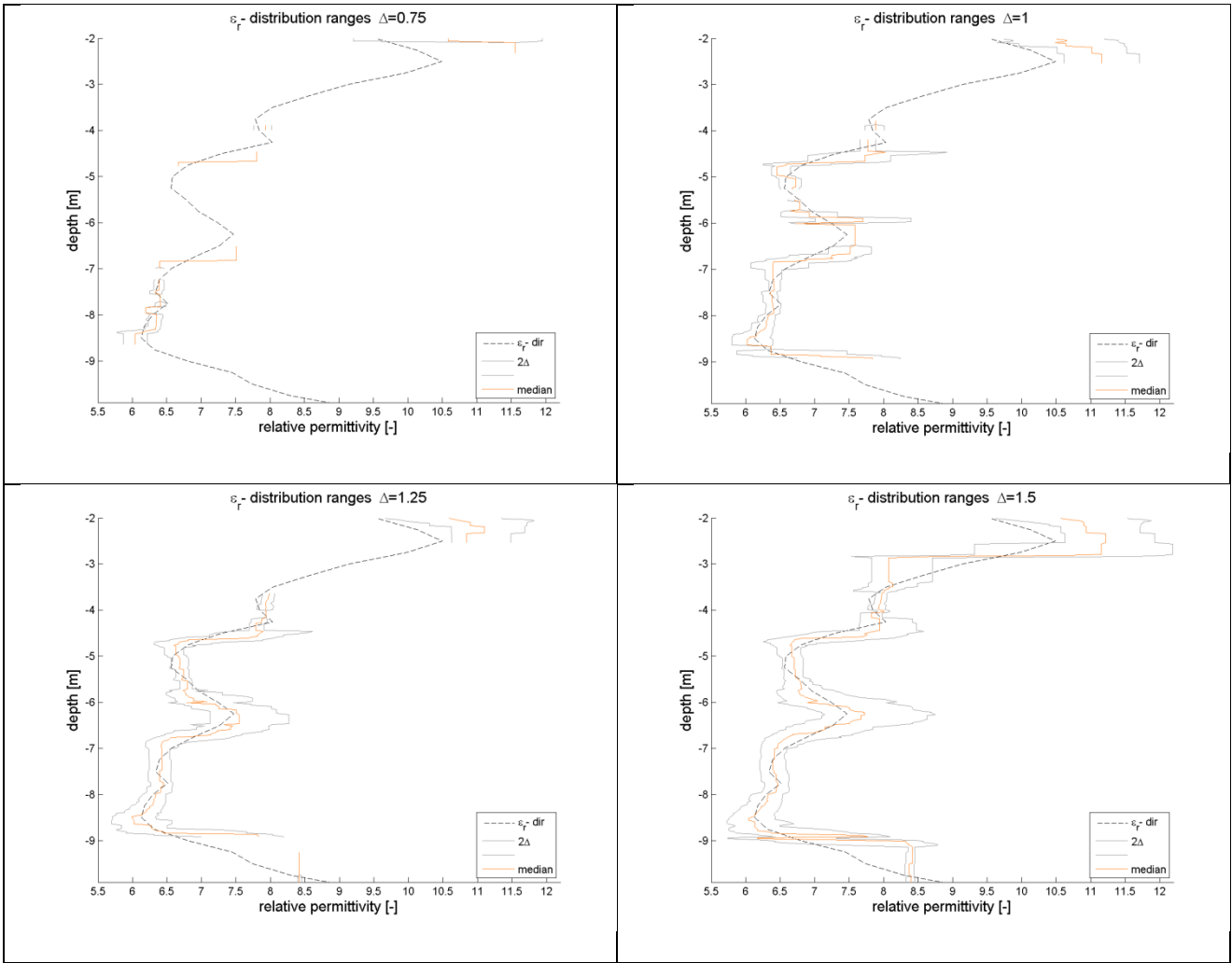


Fig. 2.5_Hatfield site dataset: different error standard deviation values (0.75, 1.0, 1.25, 1.5 ns) in the reduced chi-squared factor. Grey lines are ϵ_r -range boundaries as function of depth, accounted as two times the data standard deviation around the mean value. Orange line is the median of the data distribution, and black dashed line is the measured ϵ_r -profile from the direct-wave approach.

2.3.3 Gorgonzola field site

The second experimental dataset considered is from a field site located at Gorgonzola, few kilometres east of Milan, in the Po River valley, northern Italy. The water table at the moment of sounding, on 07 April 2005, was at -20 m depth. The unsaturated zone are composed of Quaternary sediments with a fairly coarse sand–gravel grain size distribution (Deiana et al, 2008).

Analysis of a soil core, extracted about 3 m apart the measurement boreholes, has provided direct knowledge of the site stratigraphy, two interesting features are: the presence of a 2-m-thick layer of cemented gravel and sand between -12 and -14 below ground and the existence until -6 m depth of a large fraction of fine to very fine sediments that is not observed in the deeper sediments (*Fig. 2.8*). A Pulse EKKO PE100 system was used with 100 MHz borehole antennas, which were lowered with 0.25 m vertical spacing from -3 to -18 m. Boreholes are 6.65 m apart.

The stochastic approach was applied. The geometry of the system was varied within a Monte Carlo simulation (16000 realizations), but constrained in a range of thickness and location of the layers, to maintain a link with materials analysed from the drilled core. In this case we do not reach the 20000 realizations, as in the previous cases, because the mesh dimension for the EM simulator is larger, so the computational time is very long.

Fig. 2.6 shows the ϵ_r distributions. The higher complexity of the near surface system results in a poor definition of the ϵ_r profile for 16000 realizations and an error standard deviation less or equal than 1 ns: there are present many layers with extremely sharp transitions. Nevertheless the error standard deviations of 1.25 and 1.5 ns delineate a complete ϵ_r profile with a narrow and well defined range of uncertainty (*Fig. 2.7*).

Also on this dataset, the direct-wave approach is not able to reproduce the sharper heterogeneities, the profile is rounder and smoother than emerging from the stochastic approach.

From -10 to -18 meters a large discrepancy is present between the two methods. Stochastic approach detects very sharp and defined changes in material properties, while the direct-wave method shows a very smoothed profile.

In the shallower ten meters dielectric properties change with high frequency, but with a narrow range of variability (essentially from 7.5 to 9 ϵ_r values); consequently the direct-wave and the stochastic estimations are similar. Nevertheless the larger permittivity ranges in some segment of the stochastic profile leads to an uncertain estimation of the media properties, an essential knowledge that may not be inferred from simply direct-wave analysis.

In this case the drilled core was extracted very close to the radar boreholes, so a direct comparison is possible. The core log and the ϵ_r profile from the stochastic approach, below -10 m depth, are in perfect accordance, reproducing the geometry of the system (Fig. 2.8). In particular the cemented layer between -12 and -14.5 m and the above gravel-sandy layer are perfectly defined with a sharp geometry, as evinced by abrupt changes in core lithology.

The lithological boundaries at -14.5 and -17 m are perfectly reproduced, while between this interval two different media properties are recognised. A clear and sharp permittivity limit is present at -15.5 m depth, where the core log does not report any difference in sediment stratigraphy, a physical and hydrological layering that is not direct linked with macroscopic lithology. A slightly but remarkable trend deviation is evident also in the direct-wave profile at the same depth. This phenomenon is probably caused by depositional changes, mineralogical or physical, i.e. porosity; or eventually by an extremely thin sedimentary layer, situated at about -15.5 m and that acts as a barrier for the hydrological vertical flow, raising the upper level water content.

The comparison between the geophysical inversion methods and the core log let us confident on the validity and applicability of the stochastic approach in this heterogeneous and complex subsoil system, especially for the relevant hydrogeological and hydrological information achievable from

this new application. The detection of the cemented layer, between -12 and -14.5 m, as an high permittivity material is a key point for the identification of the subsurface hydrological behaviour.

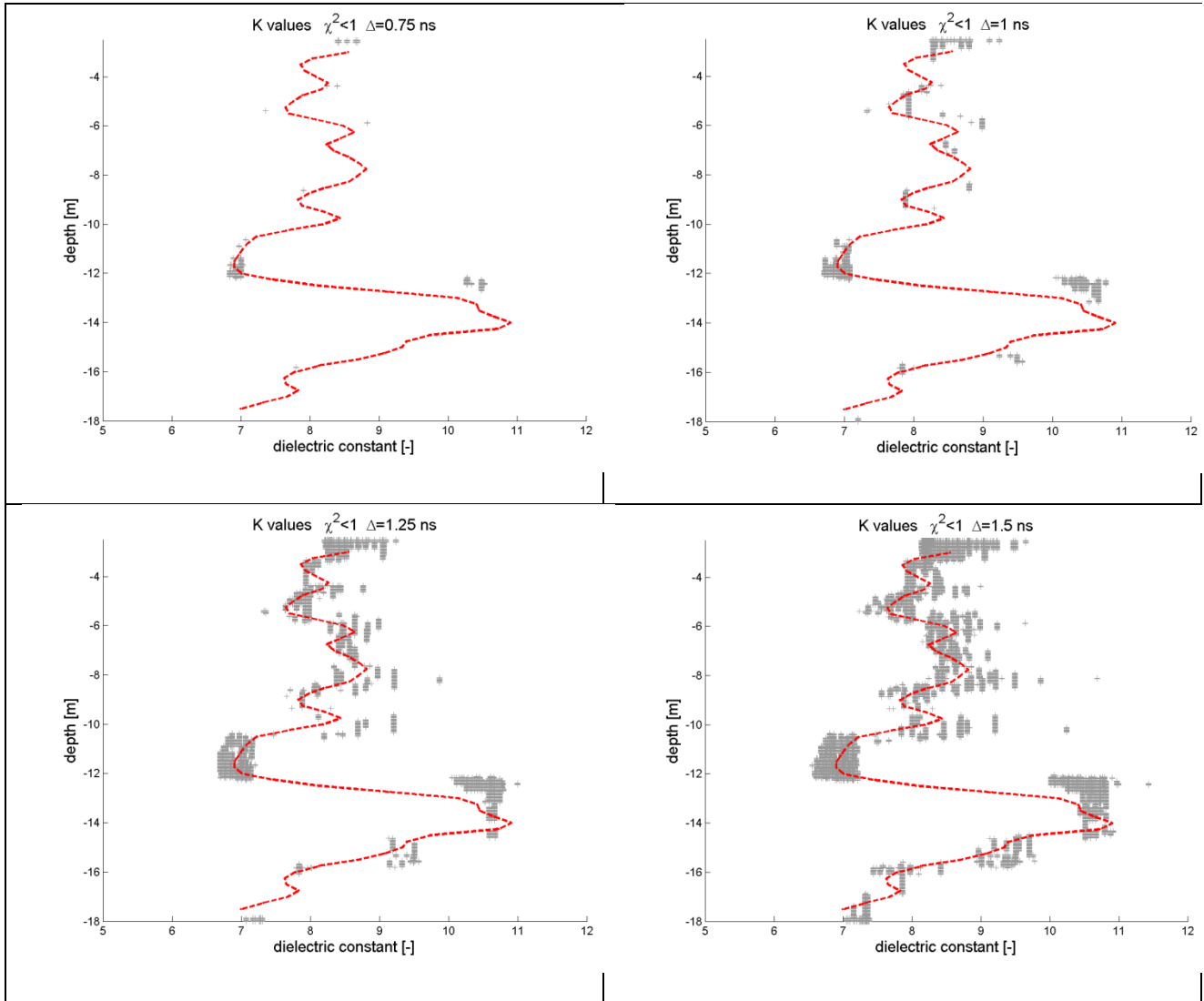


Fig. 2.6 – Gorgonzola site dataset. Distributions of ϵ_r values (light-grey crosses) after the reduced chi-squared analysis on 16000 realizations, with different standard deviation values (0.75, 1.0, 1.25, 1.5 ns). Red dashed-line is the ϵ_r profile directly obtained from experimental first-arrival travel times (direct-wave approach).

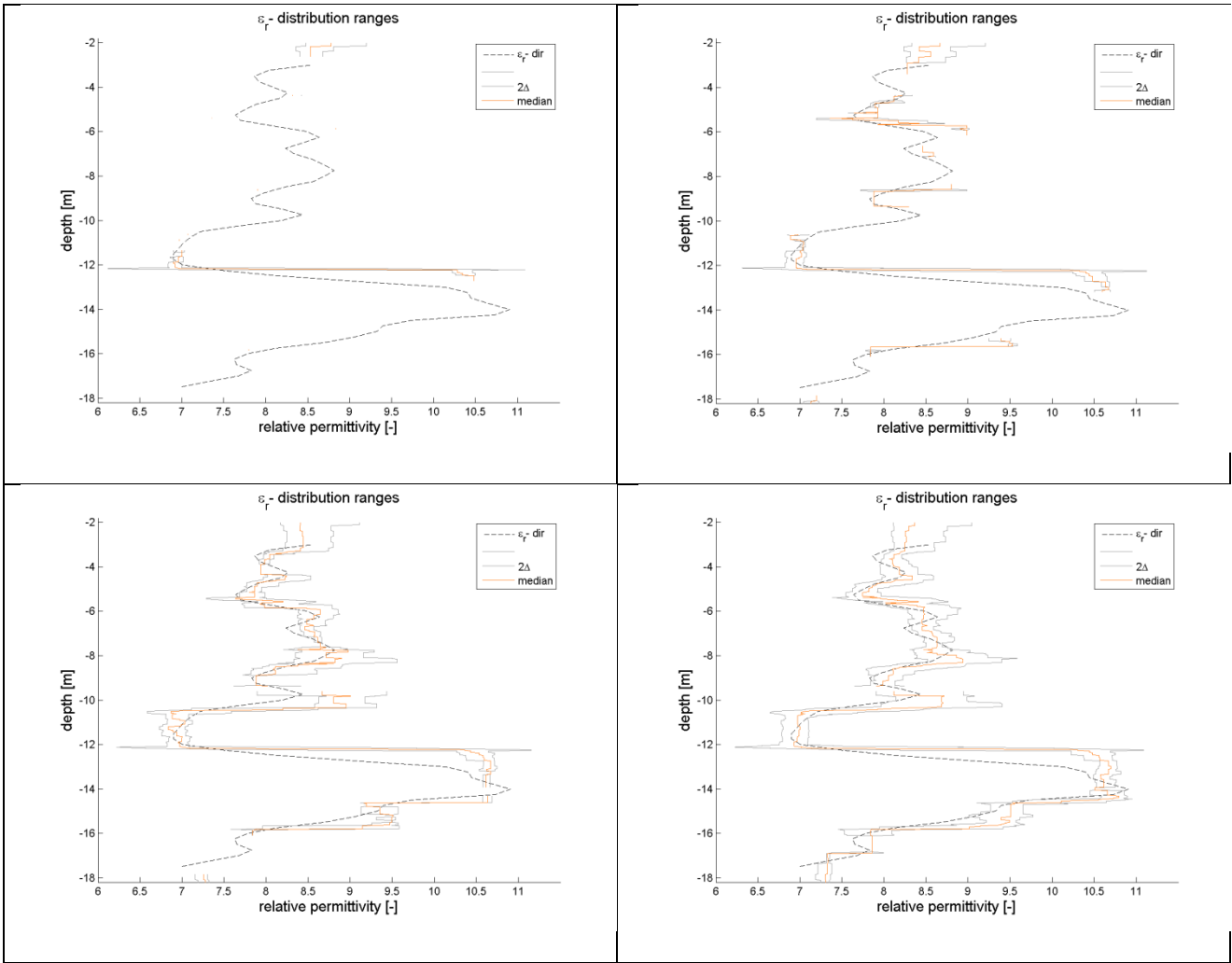


Fig. 2.7 _ Gorgonzola site dataset: different error standard deviation values (0.75, 1.0, 1.25, 1.5 ns) in the reduced chi-squared factor. Grey lines are ε_r -range boundaries as function of depth, accounted as two times the data standard deviation around the mean value. Orange line is the median of the data distribution, and black dashed line is the measured ε_r -profile from the direct-wave approach

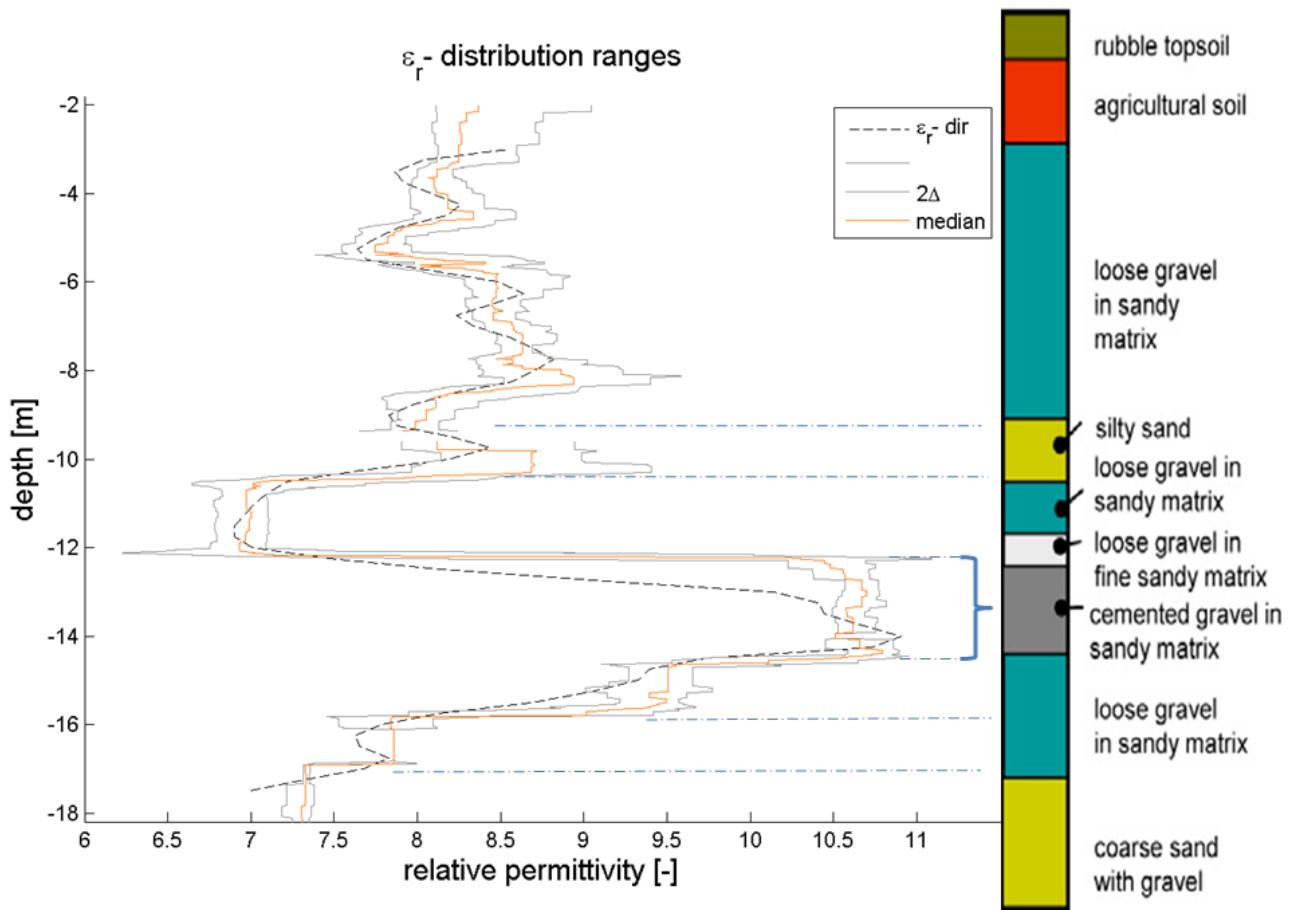


Fig. 2.8 _ Gorgonzola site dataset: comparison between the core log (on the right) and stochastic ϵ_r -range boundaries with 1.5 ns as error standard deviation (on the left).

2.4 CONCLUSIONS

An analysis, of how a cross-hole ZOP sounding could be informative of media properties, is conducted. A stochastic Monte Carlo framework is applied, with the aim of inferring knowledge about the subsoil geometry, the permittivity distribution and the related uncertainty on the physical underground system. One synthetic and two experimental field cases are analysed. The synthetic case is relevant in the validation of the stochastic approach, since the material properties, targets of the method, are a priori defined.

Both real and synthetic datasets illustrate how the often employed direct-wave approach is not able to take into account the complexity of the system. It usually reconstructs a smooth profile, sometimes underestimating the real permittivity: particularly a high ϵ_r layer might be underestimated, when it is enclosed between low ϵ_r media. Results show that care must be used inverting ZOP data for physical parameter estimation, subsurface stratification could be more complex than that apparent from direct ZOP evidences. Misleading assignment of material properties could make the evaluation significantly diverge from reality.

The evidence, from the synthetic and the experimental Hatfield datasets, is that thin layers with high permittivity values, e.g. thin clay layers or lens, are not well defined. A large uncertainty is linked to this areas which could be invisible to investigation or misinterpreted. Where the subsurface is characterized by thicker layers, both high or low ϵ_r values are well defined in a narrow uncertainty.

The comparison with core logs, in the case of Gorgonzola field site, shows a perfect match of system geometries, allowing more confidence on the validity of the analysis and on the one dimensional underground simplification.

The way hydrological parameters are deduced from geophysical data is a key point, every misleading alters the results and moves them away from the true hydraulic state of the system. The understanding of the uncertainty is essential to improve knowledge on the probable parameter distribution, ignoring thin finer layers or underestimating media properties leads to inaccurate hydrological assumptions.

3. PART II: HYDROGEOPHYSICAL INVERSION VIA TRACER TEST MONITORING

“VADOSE ZONE ‘PUSH DOWN’ EFFECT DETECTED VIA PARTICLE TRACKING ANALYSIS”

M. Rossi ¹, G. Cassiani¹, A. Binley²

¹ Dipartimento di Geoscienze - Università degli Studi di Padova

² Lancaster Environmental Centre - Lancaster University

3.1 INTRODUCTION

Hydrogeophysics is a discipline that emerged and had a great development in the last two decades. The aim of this discipline is the subsurface hydrological and hydrogeological characterization via non-invasive geophysical techniques. It can be described as the use of geophysical measurements for mapping subsurface features, estimating properties and monitoring processes that are related to hydrological studies, such as those associated with hydrogeological mapping, water resources, seepage throughout vadose zone, contaminant transport, and ecological and climate investigation.

Conventional sampling techniques, for characterizing or monitoring the shallow subsurface, typically involve collecting soil samples or drilling boreholes from which to acquire hydrological measurements. These direct measurements are typically sparsely distributed or acquired at an inappropriate scale. When the scale of the study area is large relative to the scale of the hydrological

heterogeneity or when the hydrology is complex, data obtained at point locations or within wells may not capture key information about the field-scale heterogeneity. Geophysical datasets can provide more dense 2D/3D information, are non-invasive, acquired faster and cost-effective. Associating geophysical measurements with classical hydrological measurements, it can be a great improvement in hydrogeological knowledge and hydrological processes definition.

The non-invasive investigation of the shallow subsurface to understand its hydrological and environmental properties is a very active field of research. A number of studies have appeared recently in the literature, with particular emphasis on ground-penetrating radar (GPR) (Cassiani et al. 2004b) and electrical resistivity tomography (ERT) (Binley et al., 2002). These techniques work not only as powerful imaging methods but also as means to measure changes in water saturation or solute concentration by conducting time-lapse measurements (Cassiani et al., 2004; Deiana et al., 2008). Consequently these applications can be very effective as supporting techniques for the quantification of flow and transport characteristics of soil and subsoil.

Many studies focus on the characterization of the unsaturated zone, where classical hydrological techniques are poor informative and where geophysical methods are an improving tool in hydrological parameter estimation. As it evinces from some cases, well-proved studies from literature, the vadose system must be stressed to obtain a clear and certain signal from geophysical techniques (Cassiani et al. 2005, Cassiani et al. 2009). The translation of geophysical parameters into hydrological quantities is a key issue that sometimes may be achieved only with a perturbation of the natural hydraulic state. In some cases, controlled irrigation tests and subsequently time-lapse monitoring are essential to link hydrological parameters and geophysical measurements with a reasonable degree of uncertainty.

Tracer tests in saturated media are often monitored with satisfying results, tracer plumes are usually well outlined with ERT soundings. In unsaturated subsurface the signals derived from

changing moisture content are more influential than the salinity concentration of the injected fluid. The salinity of the injected water may not be too elevated, because of the increasing density of the fluid, that as consequence drops down at higher speed. So the salinity contrast of the new water is close to the salinity of the soil moisture.

The path of a tracer in vadose zone may hence be masked from the variations of the physical status surrounding the dispersive plume; this could lead to erroneous interpretations of the evolving plume. Mass balance calculation between simulated hydraulic states and geophysical evidences may be in agreement, but both results may show a plume larger than the effective tracer fluid injected. The load of the new water, that moves under gravitational forces, produces the raising of the degree of saturation in the media just below the plume. This incidental effect could significantly contribute to geophysical signals and hydrological characterizations.

The aim of this work is the recognition and distinction of the paths of the new injected fluid from the groundwater, already present in the system and activated from pressure variations, in a sort of “piston” effect.

The discrimination between the new percolating water and the old pushed-down water is a key issue in aquifer vulnerability and soil pollution migrations, which can affect the vadose zone. Solvents and heavy metals migrations are poorly understood, due to the complexity of achieving knowledge of the unsaturated system, in spite of the high importance in contamination monitoring and in predictive dispersive paths.

So the approach adopted in this work is subdivided in two parts: the first is a hydrological parameter estimation via hydrogeophysical inversion. The hydraulic state is simulated with an appropriate finite element code and the results are validated from the geophysical monitoring evidences, in particular zero offset profile (ZOP) radar soundings. High importance is given to the characterization of the initial non-perturbed state. If high level knowledge is achieved from

geophysical data, the reconstruction of the initial steady-state is closer to reality; this is the essential input to obtain an accurate hydrological simulation.

The second part of the study is the application of a three-dimensional particle tracking code, availing of the simulated hydrological parameter evolution, i.e. flow velocities and directions on discretized times. The motion of particles in time recognizes the development of the new injected water: the shape of the plume, i.e. the centre of mass and the dispersion, may be accurately reconstructed. Also the probable position of pollutants may be achieved, both they are contained in the injected fluid or they are present in the soil and moved for the altering pressure state. A comparison is hence made with the simulated hydrological state and the geophysical data.

3.2 SITE DESCRIPTION

At the Hatfield site (S. Yorkshire, UK) an array of six boreholes were drilled in 1998 in order to monitor tracers injected into the Sherwood Sandstone (Fig. 3.1). Four of these boreholes (H-E1, H-E2, H-E3 and H-E4) were designed for 2D and 3D ERT, these boreholes were drilled to a depth of -12 m and completed with 16 stainless steel mesh electrodes. Two boreholes (H-R1 and H-R2) were installed for radar cross-hole measurements. An injection borehole (H-I2) was in addition drilled to a depth of 3.5 m and about at the centre of the geophysical arranged boreholes.

Two cored boreholes (H-M and H-AC) were drilled at the site, about 20-25 m apart from geophysical arrays and the log analysis can be find in Pokar et al. 2001. The main lithology present in the core is medium-grained sandstone, interspersed with interlaminated fine- and medium-grained sandstones, particularly in the zone around -6 m depth, and between -8 and -9 m. Drift at the top of the section at the site is typically 2–3 m thick, and consists mainly of fluvio-glacial sands.

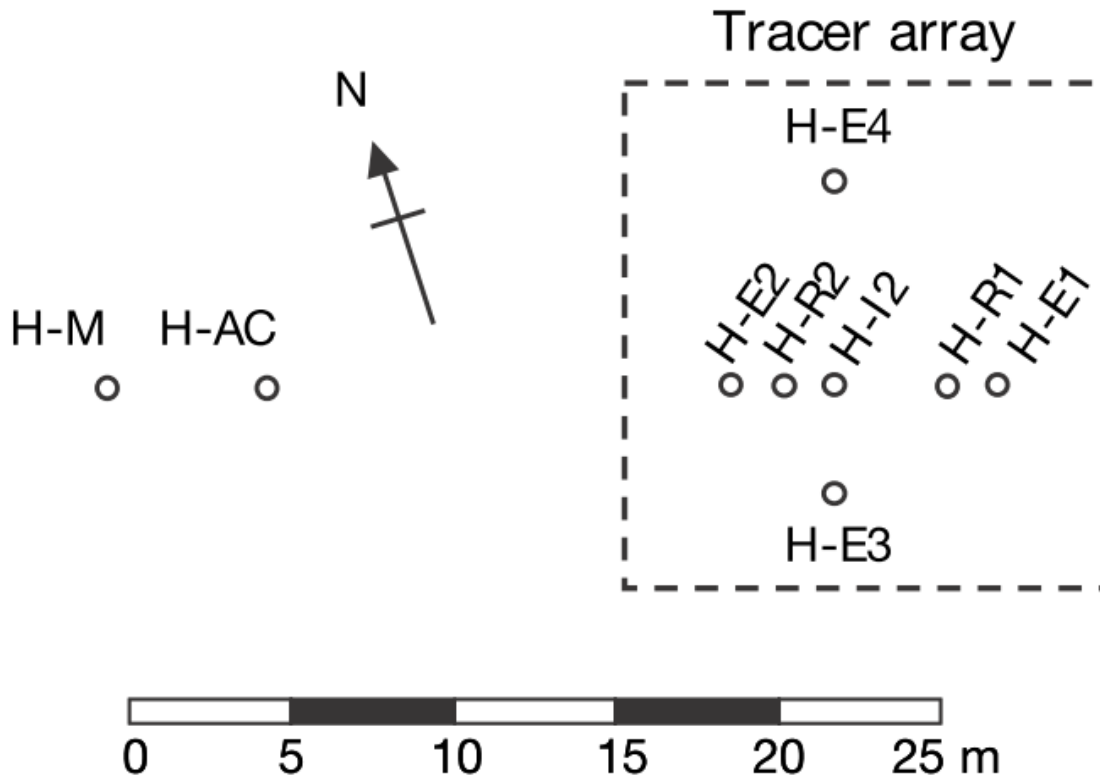


Fig. 3.1 _ Field layout with installed boreholes locations.

3.3 MONITORING TRACER INJECTION TEST

During March 2003 a saline tracer was injected into the sandstone using borehole H-I2. Changes in bulk resistivity and dielectric constant of the sandstone were then monitored using cross-borehole radar and ERT (Winship et al., 2006). Radar soundings were performed with a Sensors and Software Pulse EKKO PE100 system (Sensors & Software, Mississauga, ON, Canada) and 100 MHz antennas. In the ZOP sounding the antennas were lowered at 0.25 m increments from -2 to -10 meters below the surface. In this work we focus on ZOP cross-hole radar, high informative on mono-dimensional moisture variations, to validate simulated hydrological models; while ERT and multiple offset gathers (MOG) surveys are applied in the comparison with the particle tracking results.

The tracer consisted of 1200 l of water, dosed with NaCl to give a density of 1001.67 g/m³ and an electrical conductivity of 2200 μS cm⁻¹ (groundwater conductivity measured at the site was 650 μS cm⁻¹). The saline tracer was injected over a period of 3 days, from 14 to 17 March 2003, at a steady rate of approximately 17 l h⁻¹. The flow was monitored to give the precise cumulative injection volume over time. The water table was observed at approximately 10 m depth.

3.4 HYDROLOGICAL MODELS

3.4.1 Initial steady water flow state

Great emphasis was given to the characterization of the initial, pre-injection, steady-state. The quasi-steady water flow is confirmed from the geophysical soundings, that show very similar responses during the monitoring of the two months before the tracer test, especially in the portion below 3.5 m depth, where the injection is set.

The knowledge on the initial state is the essential input to start an hydrological simulation that is able to reproduce the evolving characteristics of the system during the water injection. If the steady-state flow is not described with a good accuracy, the results of the simulations could diverge from reality, also if the hydrological state shows a good match with geophysical evidences.

Many tries had initially be done on the easiest direct derivation of permittivity from ZOP travel time velocities (v):

$$— \tag{3.1}$$

where ϵ_r is the bulk relative dielectric permittivity (or bulk dielectric constant) of the medium itself and c is the radar wave velocity in air (0.3 m/ns). The steady-state moisture content profile was employed in several 3-D hydraulic finite element simulations, varying the state parameters in a broad range. The results show a not stable initial state: percolations were observed in some areas

before the injection. So a statistically-based analysis became crucial in the preliminary properties estimation.

In a previous study (see chapter 2) the background ZOP data are analyzed to obtain a one-dimensional relative permittivity profile. For this purpose an electromagnetic wave simulator has been applied within a stochastic Monte Carlo framework, in this manner both averaging and critically refracted wave effects are taking into account. Results from synthetic and real ZOP datasets are statistically analysed to deduce what kind of subsoil permittivity distributions are resolvable and well defined with a degree of uncertainty (Fig. 3.2).

On the basis of the stochastic approach a permittivity distribution is fixed. The ϵ_r profile is subdivided in homogeneous layers, where media are identified in an alternating sequence of medium and fine sandstone with the same frequency that evinced from core logs. So the subsoil is subdivided in several layers, combined in only three different media: the upper sandy soil (drift) until a depth of -2 m (media 1) and the underlying alternating sequence of the Sherwood Sandstone, fine (media 2) and medium (media 3) grained materials as synthesized in Fig. 3.3 and Fig. 3.2.

The relative permittivity of each layer is then easy linked to moisture content with the application of the semi-empirical complex refractive index method (CRIM) (Roth et al., 1990):

$$\epsilon_r = \epsilon_{gr} + \frac{\epsilon_w - \epsilon_{gr}}{1 + \epsilon_w} V_p \quad (3.2)$$

where ϵ_{gr} is the permittivity of the sediment grains, ϵ_w is the permittivity of water (assumed to be 81 [-]), ϵ_{air} is the permittivity of air (assumed to be equal to 1 [-]) and V_p is porosity. ϵ_{gr} is fixed at a value of 5 [-], since it is appropriate for the main lithological unit of the core and for 100 MHz frequency measurements, as it is shown by West et al. (2001).

The derivation of dielectric property in moisture content requires a saturated moisture content estimation. Further knowledge on the initial hydrological steady-state is then necessary before

starting with a hydrological simulation, i.e. unsaturated Van Genuchten parameters (Van Genuchten, 1980). These information are not achievable from non-invasive measurements, so an estimation is needed.

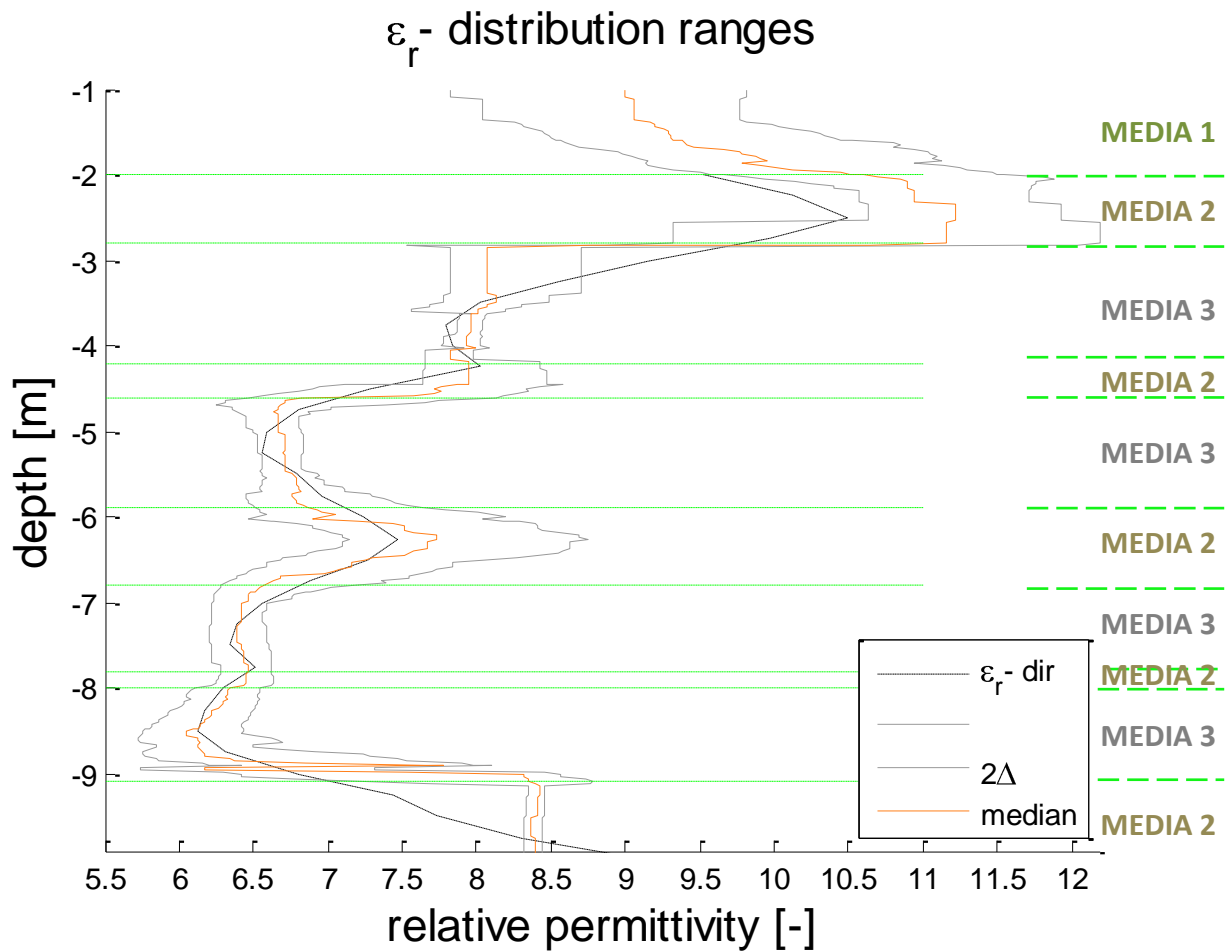


Fig. 3.2 _ Hatfield steady-state conditions from stochastic approach. Grey lines are ϵ_r -range boundaries as function of depth, accounted as two times the data standard deviation around the mean value. Orange line is the median of the data distribution, and black dashed line is the measured ϵ_r -profile from the direct-wave approach (eq. 3.1). On the left is reported the chosen layers subdivision.

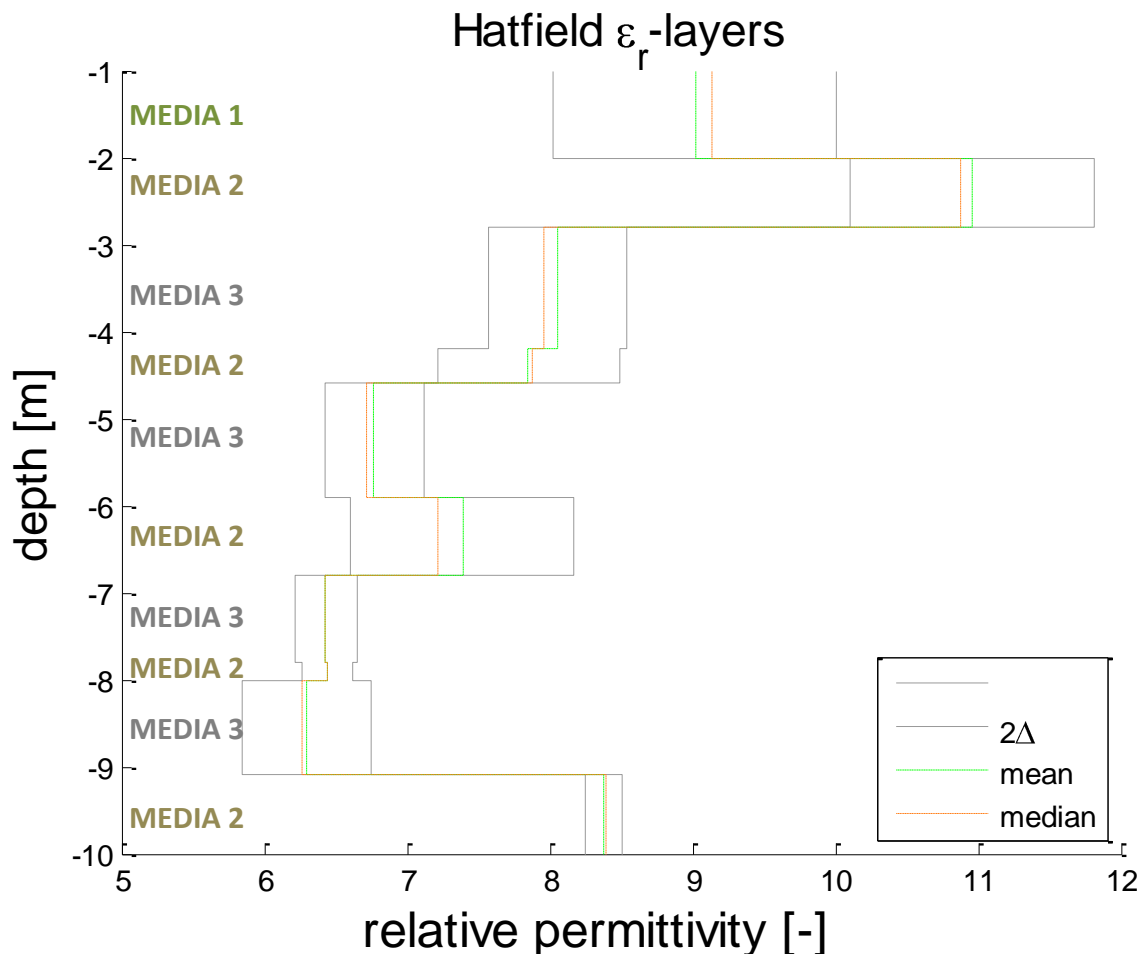


Fig. 3.3 _ Vertical mono-dimensional layers subdivision with statistical illustration of the permittivity distribution, achieved from stochastic approach. On the right is reported the media alternating sequence.

3.4.2 Selection of the hydraulic parameters

At this point a stochastic approach is adopted, via the semi-analytical hydrological simulator *ss_infil* (Rockhold et al., 1997), where the hydrological parameters are made to vary inside the pervious predetermined layer positions and locations (Fig. 3.3). The choice of the semi-analytical code is necessary, due to the faster computing time respect to a finite element software; as consequence, a broad range of parameters distribution may be explored. The code implements an integral solution for one-dimensional steady vertical water flow in layered soils with arbitrary

hydraulic properties: K_s , saturated hydraulic conductivity [L/T^{-1}]; θ_r , residual moisture content [L^3/L^3]; θ_s , saturated moisture content [L^3/L^3]; van Genuchten model α parameter [L^{-1}]; van Genuchten model n parameter [-]. For this model, the adopted logarithmic hydraulic conductivity function must be discretized in a number of piecewise-linear curve segments. In this work 50000 segments are employed. For the natural steady flow conditions the mean net infiltration rate is adopted: 3.5×10^{-4} meters/day, based on rainfall data and actual evapotranspiration estimates over the period of monitoring at the site.

Two millions of realizations are run in a Monte Carlo framework with parameters randomly sampled from appropriate ranges of variability, in according with literature values for site materials. Tab. 3.1 shows the parameter ranges adopted in the stochastic model. The large number of realizations is essential, since an hydrological quantity could differently influence the system if associated with others properties; so an extended exploration of the multi-dimensional parameter space is achieved.

Fixed the saturated moisture content magnitude, i.e. the porosity, the natural moisture content profile is calculated using CRIM (eq. 3.2) and including the permittivity distribution from the prior stochastic analysis on the ZOP dataset (Fig. 3.3).

At each realization of the stochastic framework, the semi-analytical code returns a mono-dimensional profile of moisture content, that at this point could be compared with the input moisture content distribution: closer the degrees of saturation are, more stable is the system and more reasonable the simulated Van Genuchten parameters array. To evaluate the goodness of fit the statistical efficiency index (or Nash–Sutcliffe model efficiency coefficient; Nash and Sutcliffe, 1970) is calculated between the initial and the final moisture content profile:

$$(3.3)$$

where θ_f is the final moisture content profile resulted from the *ss_infil* model, θ_i is the initial moisture content profile used as input in the model and achieved from the stochastic analysis of the background ZOP sounding, σ^2 is the variance of the moisture content distribution. The E is an index that can vary from $-\infty$ to 1. An efficiency of 1 ($E = 1$) corresponds to a perfect match of modeled discharge to the observed data.

VAN GENUCHTEN PARAMETERS	MIN VALUE	MAX VALUE
K_s [m/d]	0.04	1.4
θ_r [-]	0.03	0.1
θ_s [-]	0.25	0.35
α [m⁻¹]	0.1	2
n [-]	1.5	2.5

Tab. 3.1_ Ranges adopted in the stochastic framework for the Van Genuchten parameters.

In this work the best efficiency indexes are around -80, that are not very good values. Anyway it must be noticed that the efficiency is a severe indicator of the goodness of fit and that it is an useful tool to select those models that are closer to reality. In Fig. 3.5 the two millions Van Genuchten parameters for the media 3 (medium grained Sherwood Sandstone) are plotted versus the efficiency index. Similar results are achievable for the two remaining media. It is clear that some parameters

are better defined with this analysis and that ranges of variability may be restricted: θ_s , α , n . The other parameters show sparse clouds in the scatter plot: no restrictions are possible, so the goodness of fit should depend on the singular parameter combination and on the interaction of the hydraulic properties.

An analysis on the correlation of the best 500 realizations of Van Genuchten parameters (lower efficiency coefficients) is pursued via the principal component analysis (PCA). The result shows that no correlations are present between the parameters and the efficiency index, as it is clear from the *scores plot* (Fig. 3.4).

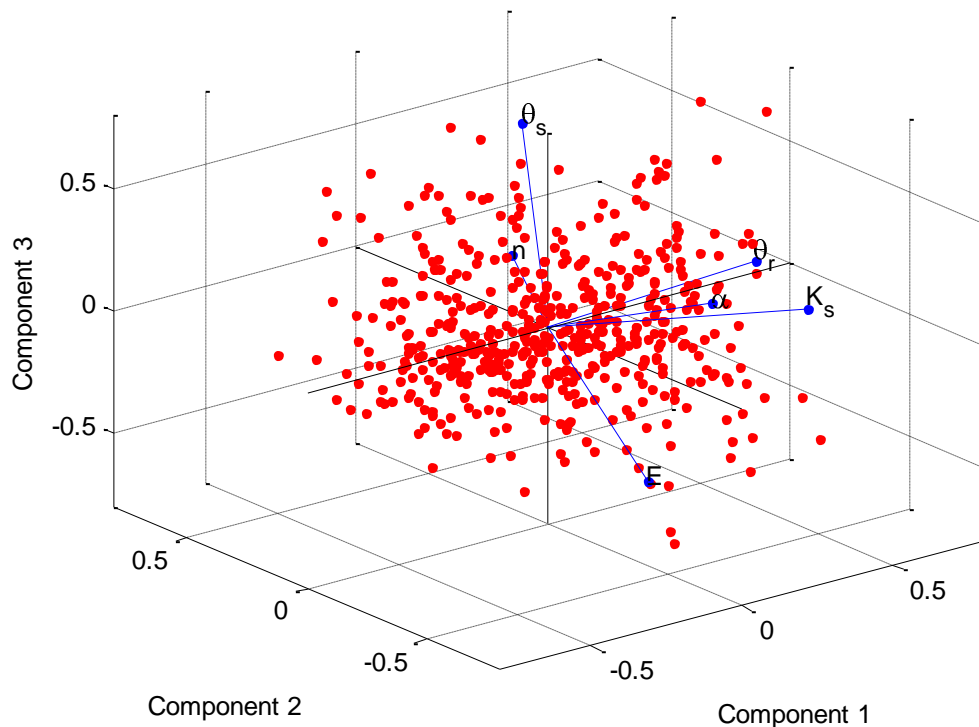
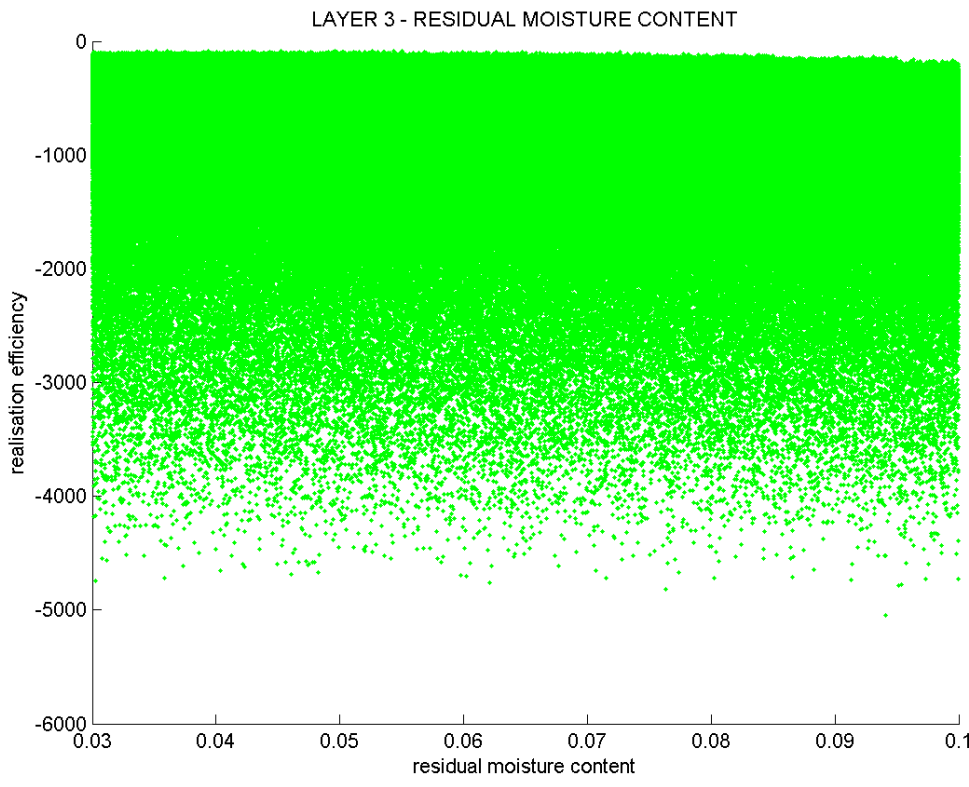
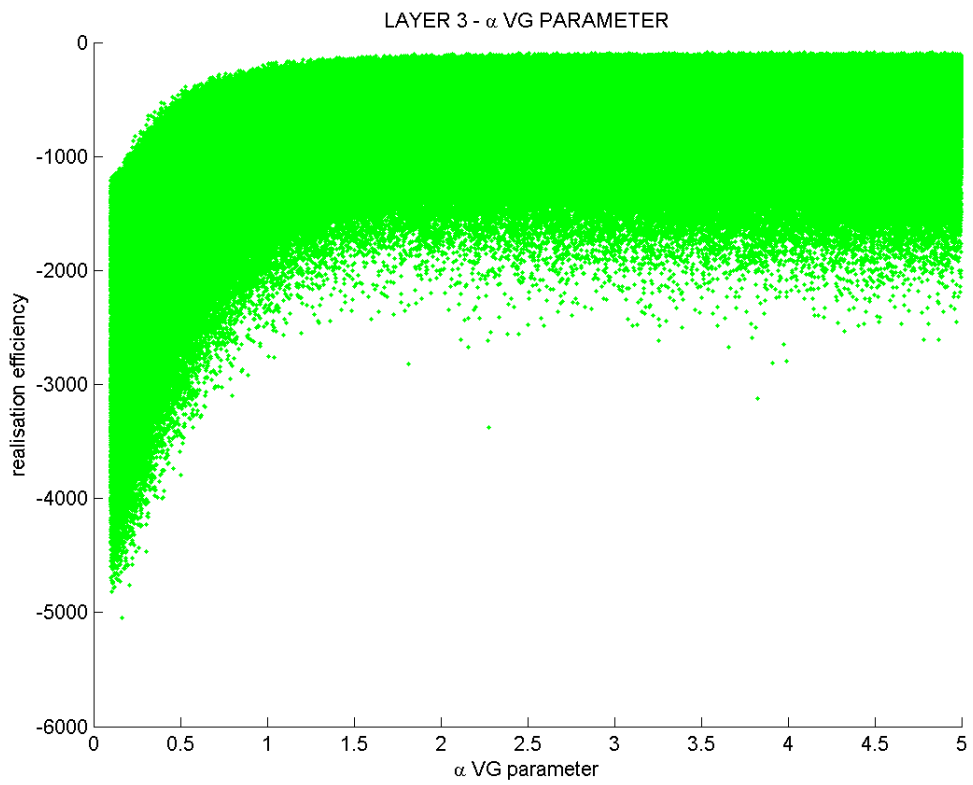
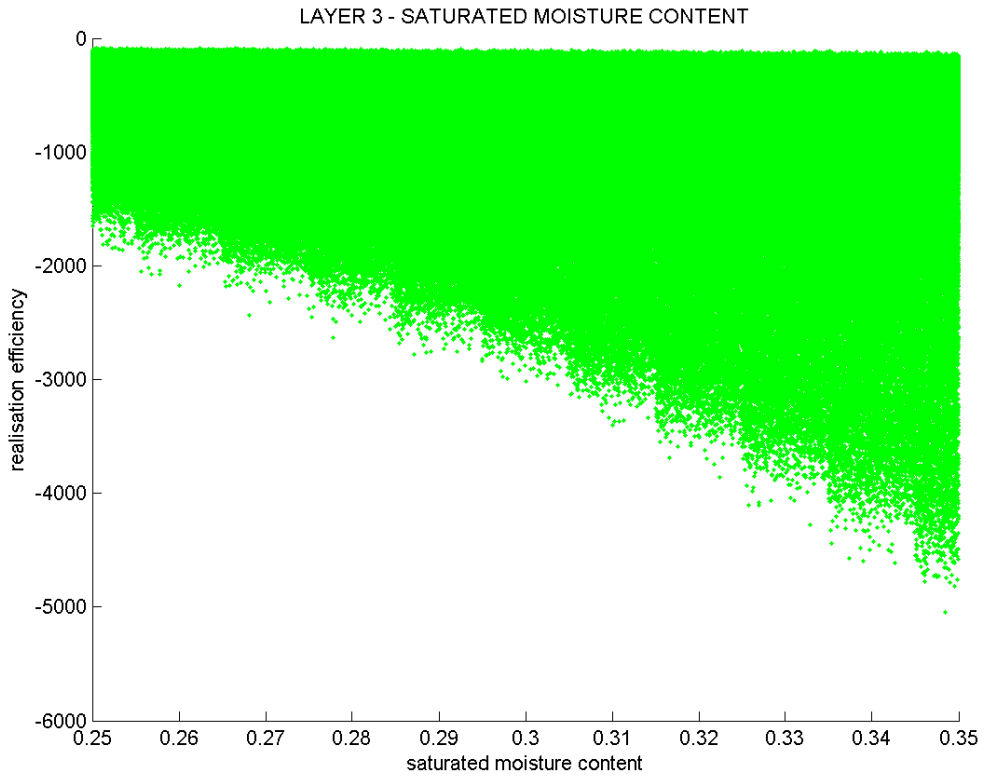


Fig. 3.4 _ Scores plot resulting from the PCA on the best 500 realizations, selected by the efficiency coefficient (eq. 3.3) and obtained from the Monte Carlo framework on the semi-analytical hydrological model (*ss_infil*).

This method is helpful to recognize those parameter combinations that are linked to a steady vertical water flow, the necessary starting point for an hydrological model able to follow the progress of an injected tracer. The best realizations, in term of efficiency index values, are selected for a further analysis: the three-dimensional finite-element hydrological simulations, able to reproduce the tracer injection and evolution in the vadose subsurface.





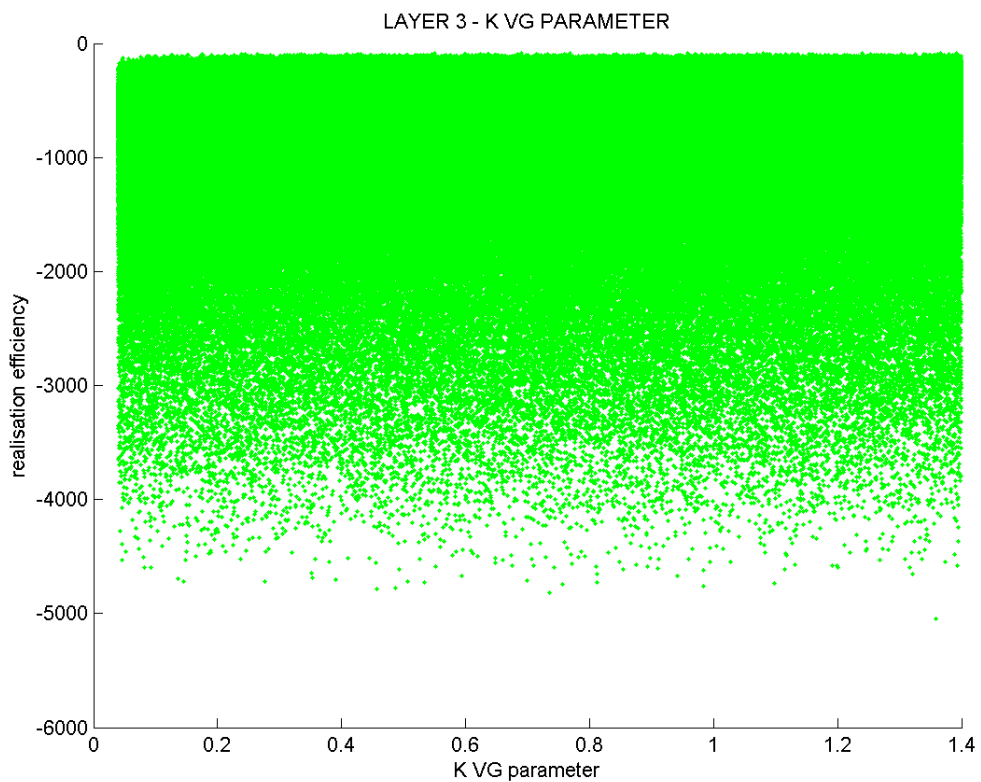
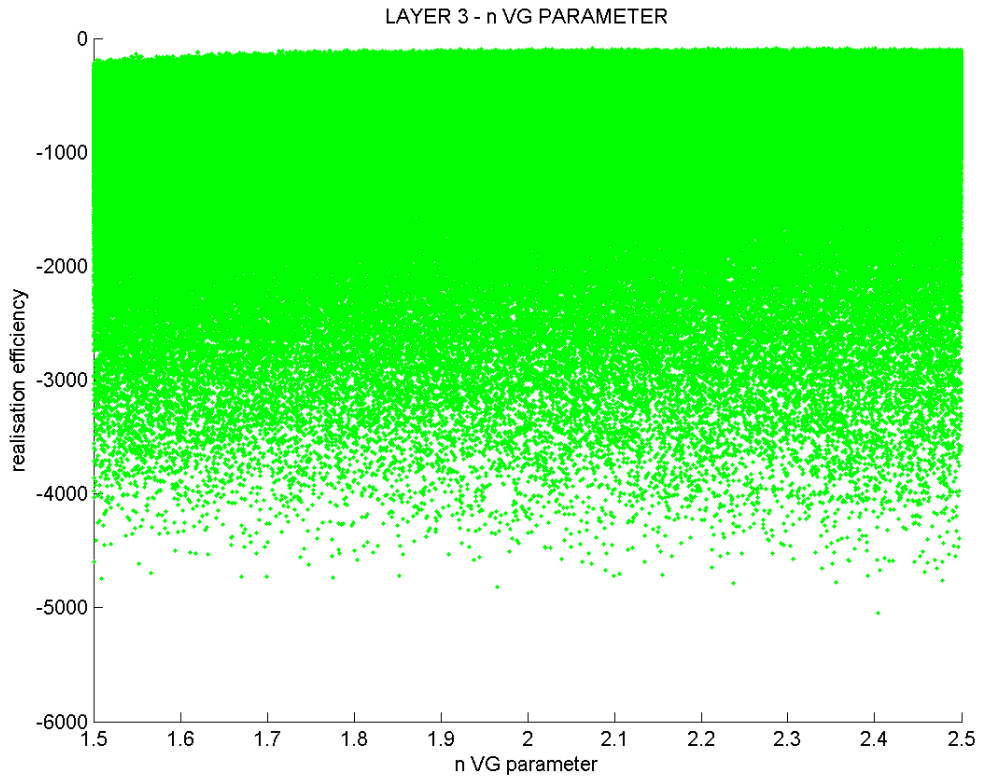


Fig. 3.5 _ Two millions Van Genuchten parameters for the media 3 (medium grained Sherwood Sandstone) plotted versus the efficiency coefficient.

3.4.3 Tracer injection simulations

The best 100 arrays of hydraulic parameters are taken into account for further analysis. For every selected array of the hydraulic parameters, the three-dimensional finite-element hydrological simulator FEMWATER (Lin et al., 1997) is run. In FEMWATER, the Van Genuchten model (Van Genuchten, 1980), describing the relationships among unsaturated hydraulic properties, is adopted. The vadose physics are described by the following relationships:

$$(3.4)$$

and

$$(3.5)$$

where ψ is the pressure head and S_e is effective saturation [$S_e = (\theta - \theta_r) / (\theta_s - \theta_r)$].

A model was set up to represent a parallelepiped of 11 m x 11 m in plan, to allow specification of zero horizontal flow-boundary conditions, and 10 m in depth, since the water table measured just before the tracer test was at about -10 m depth. The mesh model was composed of 195112 six-node prism elements and 101054 nodes. The system was obviously composed of the same vertical geometry adopted in the semi-analytical code (Fig. 3.3). The injection took place in the coarser sandstone material at -3.5 m depth. The solution to the system of non-linear equations was achieved with a convergence threshold for hydraulic head equal to 0.001 m. The total simulation time was 362.6 h, coinciding with the last ZOP monitored survey.

FEMWATER is based on a pressure head formulation, so the initial pressure head at each node of the mesh is required. It is calculated with eq. 3-4 from the one-dimensional moisture content profile and the fixed hydraulic properties for that specific simulation.

3.5 HYDROGEOPHYSICAL MONITORING

The hydraulic 3-D simulations produce an evolving dynamic state, that must be corroborated by some experimental measures in order to validate the calculated parameters with the real physics of the system. For this purpose the time-lapse geophysical measurements are taken into account.

The field plume dynamics were monitored with ZOP soundings at several time-steps. For every single time-step the moisture content profile was calculated from the hydrological model. At this point the possible approaches are fundamentally two:

a) Geophysical inversion approach

- translate the geophysical quantities from ZOP surveys, i.e. relative permittivity, in measured moisture content profiles with the petrophysical relationship accounted in eq. 3.2;
- extract an averaged one-dimensional moisture content profile from simulated hydraulic quantities distribution;
- calculate the goodness of fit between the two moisture content profiles.

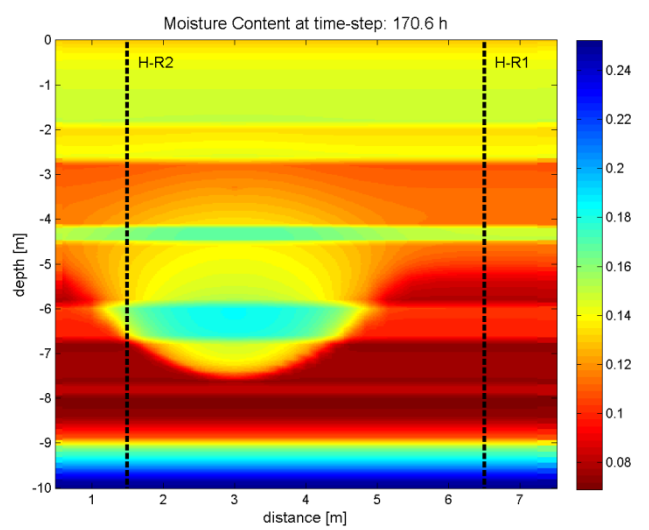
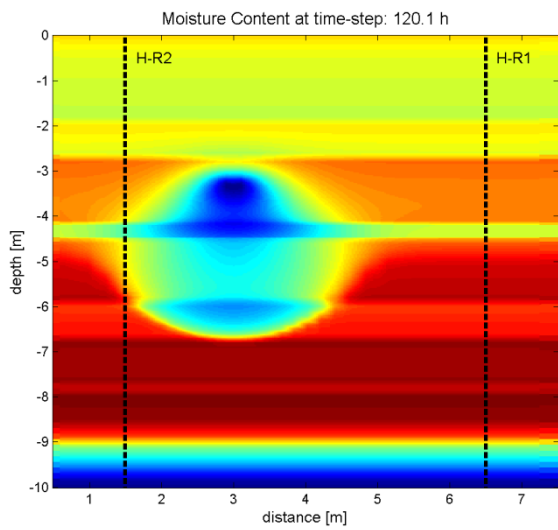
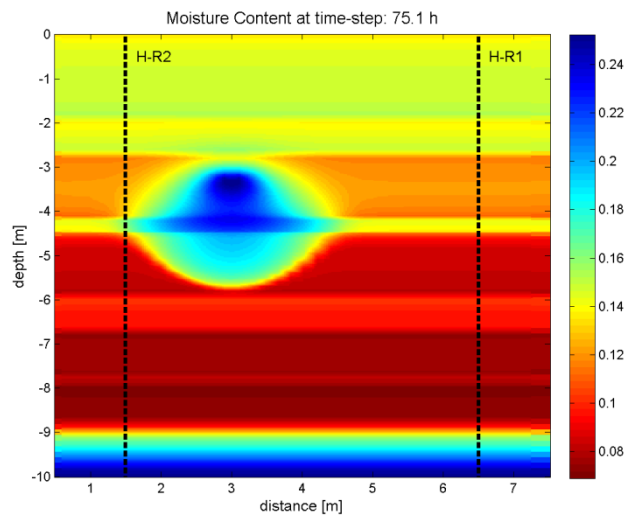
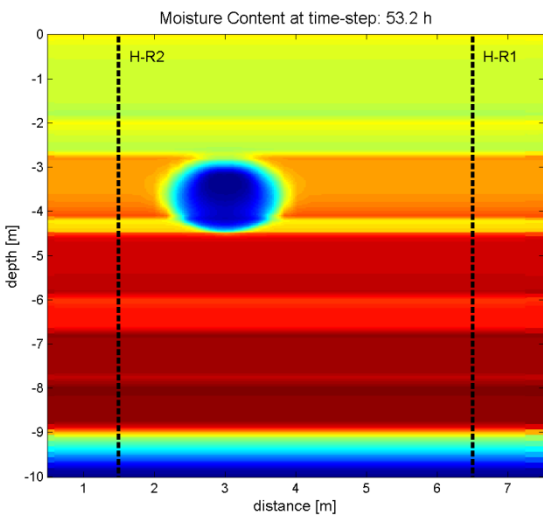
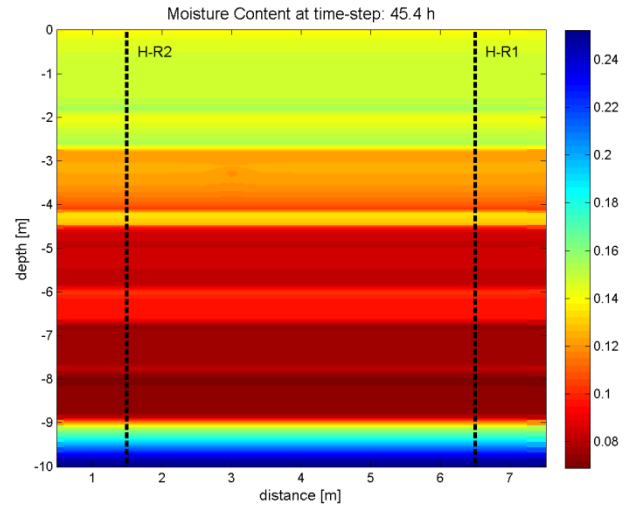
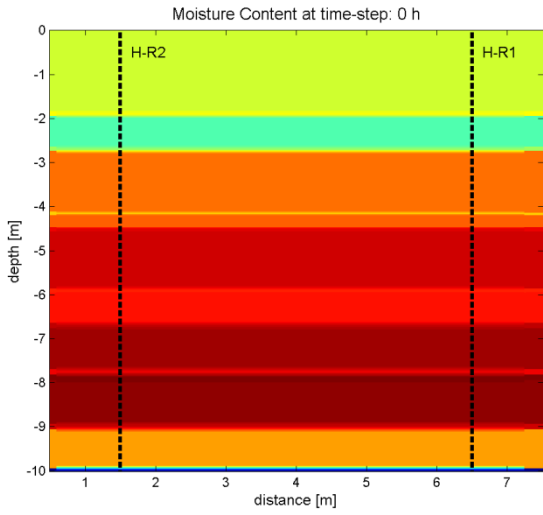
b) Geophysical forward model approach

- extract the hydrologically-simulated moisture content 2D-distribution between the GPR boreholes;
- translate the calculated moisture content distribution in a relative permittivity distribution with the application of the CRIM petrophysical relationship (eq. 3.2);
- run an electromagnetic (EM) simulator to obtain the forward model;
- calculate the goodness of fit between the measured dataset and the calculated dataset.

These different approaches are summarized in Fig.1.1 and Fig. 1.2, respectively.

The usage of the first method, directly deducing the dielectric property distribution from radar travel times, could lead to misleading due to critical refraction and averaging effects, as it is demonstrated in chapter 2. So the advantage of the second approach is the possibility of a direct comparison with the acquired first-arrival travel times, without the requirement of the conversion of these data. As consequence, the calculated velocities could be the result of a properties distribution that cannot be achieved from the direct-wave approach. Nevertheless, as explained in the previous work (see chapter 2), some material distributions could not be reproduced: there are layers that are quasi-invisible at the first-arrival travel times analysis, due to the singular electromagnetic wave propagation paths that do not involve, or only partially involve, these media.

The approach adopted in this work is the second method. So, from the 3D hydrological model, the moisture content distributions are extracted at precise time-steps, which coincide with ZOP surveys timing. For each time-step a 2D moisture content distribution is obtained, interpolating the 3D distribution on a 2D vertical plan, that includes the exact locations of the GPR boreholes (see Fig. 3.6). The moisture content values are then translated in relative permittivity with the semi-empirical CRIM relationship (Roth et al., 1990) (eq. 3.2), including the saturated moisture content profile set for that specific FEMWATER simulation. At this point the ϵ_r distribution is used as input for an EM simulator, where the measuring survey is reproduced. The adopted EM wave propagation simulator is a finite-difference time-domain MATLAB code by Irving and Knight (2006). The modelled survey geometry reflects the measured ZOP sounding: transmitter and receiver 100 MHz antennas were simultaneously lowered at 0.25 m increments from -2 to -9.5 metres below the surface. The modelled receiver responses are then employed for the picking of the first-arrival travel times.



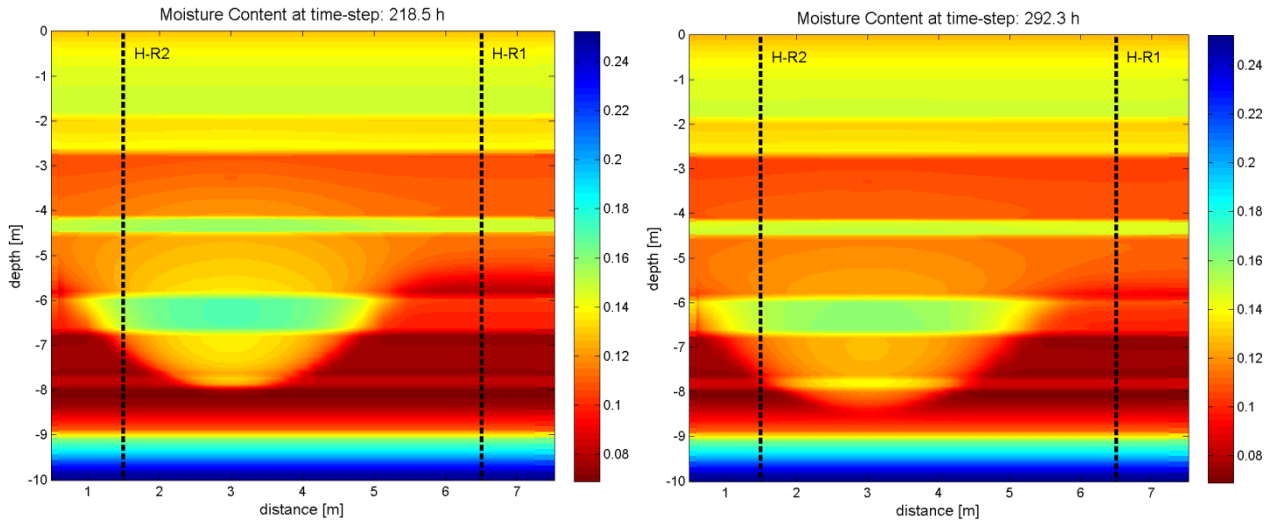
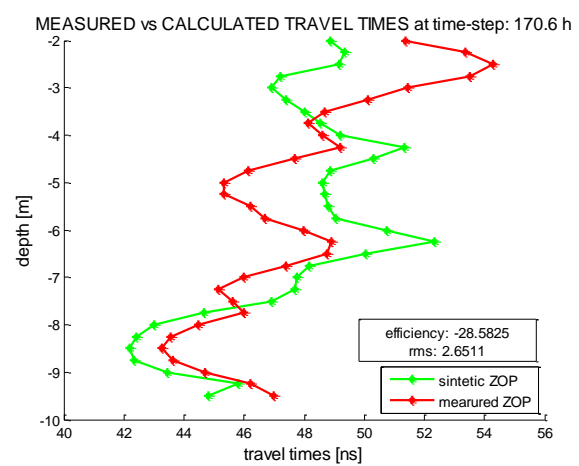
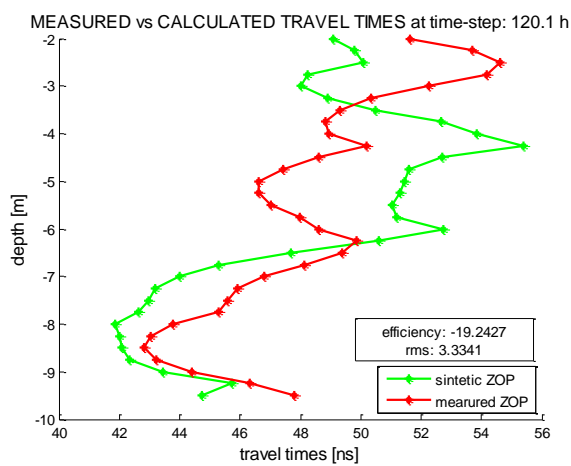
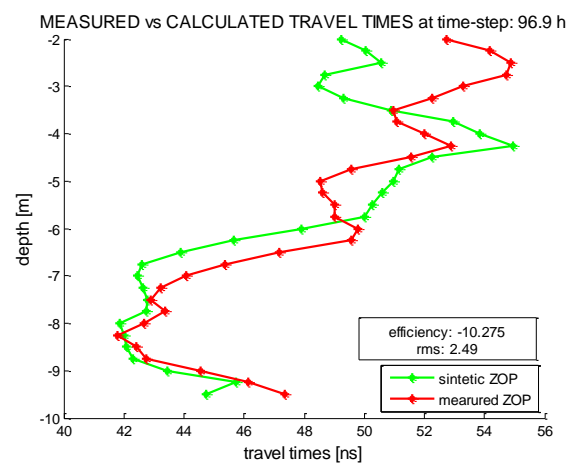
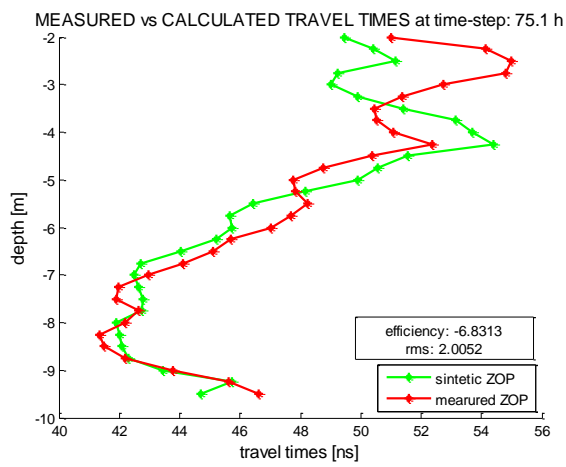
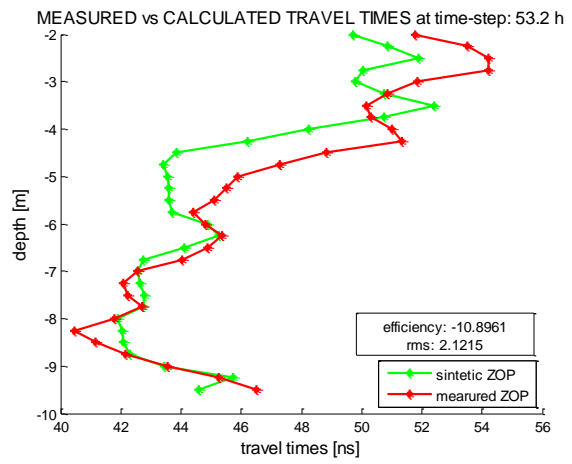
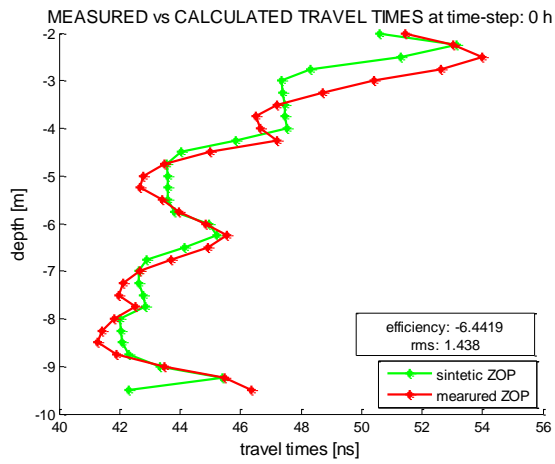


Fig. 3.6 _ The moisture content distribution achieved from the hydrological model. The 2-D representation is extracted on the vertical plan that intersects the boreholes equipped for the GPR measurements: H-R1 and H-R2. It is clearly visible the tracer plume evolution in time.

At this point a comparison between the calculated and the measured travel times is done via the efficiency coefficient calculation, as exposed in eq. 3.3, but this time using travel times quantities in spite of moisture content (fig. Zop_confr). These results lead to an accuracy estimation of the simulated hydrological model: closer the calculated and the measured ZOP datasets are, more realistic are the simulated hydraulic parameters. This method is helpful to recognise those simulated hydraulic systems that are able to reproduce the real properties distributions, for an estimation of not-directly measurable quantities.



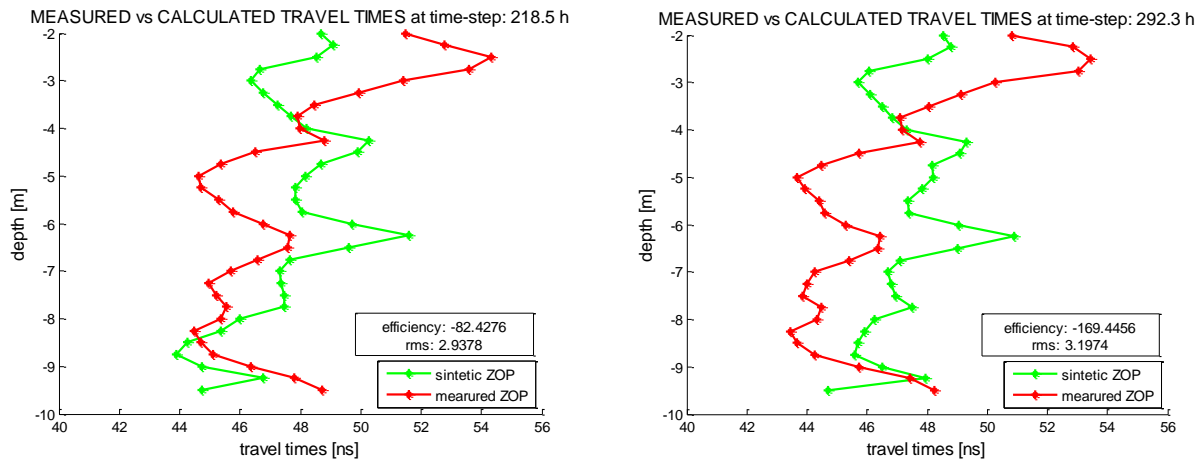


fig. Zop_confr _ Comparison between calculated and measured ZOP travel times profiling at different time-steps, during the monitored tracer injection test, reporting the efficiency and root mean square indexes.

3.6 PARTICLE TRACKING ANALYSIS

Chosen the hydraulic simulation that better matches the real subsurface system with the aim of the hydrogeophysical inversion, a particle tracking analysis is applied to the evolving subsoil model.

A particle tracking code, written in MATLAB, reads the outputs of the FEMWATER hydraulic software at different time-steps. Time-steps must be short enough to avoid the loss of information in the developing hydrological state: a time interval of 2 hours is established.

Particles are generated at the surface of injection, at -3.5 meters from ground surface (the base of the H-I2 borehole, see Fig. 3.1), in a fraction that is depending on the measured water flux during the experiment. Each particle has the same weight, that is a consequence of the total number of particles and the entire amount of injected tracer; so if the flux rate changes, the number of particles adequately varies. For this analysis 10'000 particles are employed.

The particles are then moved in the three-dimensional space on the basis of the flux velocities extracted from the FEMWATER outputs. In this way tracer paths may be monitored and the exact evolution of the new water plume may be achieved.

A subsequent comparison with the 3D inverted ERT datasets and 2D inverted MOG dataset at every time-step is done. The resistivity, achieved from the 3D ERT inversion, may be shown the tracer plume evolution in time. The centre of mass of the particles may be compared with the centre of resistivity variation respect to background dataset. In the 3D volume it could also be calculated the dispersion of the particles and of the resistivity changes, if the variations of resistivity respect to the background survey are achieved. The same comparison may be done on the 2D inverted MOG radar datasets, looking at the centre and the spreading of the dielectric property variation respect to the background.

3.7 RESULTS AND DISCUSSION

The applied methodology is projected for the hydrological characterization of the vadose subsurface zone in an experimental field. The accuracy, regarding the characterization of the pre-injection physical state, is a focal point, essential for a following plausible hydrological model. Also without a previous work on the steady water flow description, the hydrological properties may be estimated via an hydrogeophysical inversion; nevertheless a restriction on the starting modelled hydrological parameters is a key point in the validation and corroboration of the simulated physical state. The stochastic approach leads to satisfactory results in the hydrological model able to reproduce the true physical state.

Furthermore the particle tracking analysis shows interesting results. The subsoil system shows a push-down effect during the tracer injection, as it evinced by the comparison between the

hydrological model, the two- and three-dimensional ERT inversions, the two-dimensional MOG inversions and the particle tracking evolution.

Both ERT and MOG imaging reproduce the true hydraulic state, taking into account the different resolutions of the techniques. The hydraulic synthetic model is close to that

The discrimination of the new injected water from the old water, already present in the ground and moved under varying pressure forces, may interestingly be informative on the waste hazards and pollutant migrations.

3.8 CONCLUSIONS

The applied methodology is projected for the hydrological characterization of the vadose subsurface zone in an experimental field. The accuracy, regarding the characterization of the pre-injection physical state, is a focal point, essential for a following plausible hydrological model. Also without a previous work on the steady water flow description, the hydrological properties may be estimated via an hydrogeophysical inversion; nevertheless a restriction on the starting modelled hydrological parameters is a key point in the validation and corroboration of the simulated physical state. The stochastic approach leads to satisfactory results in the hydrological model able to reproduce the true physical state.

Furthermore the particle tracking analysis shows interesting results. The subsoil system shows a push-down effect during the tracer injection, as it evinced by the comparison between the hydrological model, the two- and three-dimensional ERT inversions, the two-dimensional MOG inversions and the particle tracking evolution.

Both ERT and MOG imaging reproduce the true hydraulic state, taking into account the different resolutions of the techniques. The hydraulic synthetic model is close to that

The discrimination of the new injected water from the old water, already present in the ground and moved under varying pressure forces, may interestingly be informative on the waste hazards and pollutant migrations.

4. CONCLUSIONS

The present work is an example of the hydrogeophysical inversion methods, where great emphasis is focused on the characterization of the hydraulic state preceding the tracer injection test. Anyway the system must be stressed under artificial hydraulic states to force the parameters estimation and to limit the range of probable hydrological models. Also under these condition an uncertainty on the hydrogeophysical inversion method must be considered, due to the challenging issue: the measured geophysical data are subjected to experimental errors, the resolution of the geophysical techniques is limited, the a priori knowledge on the site hydrogeology is imperfect, the complex three-dimensional hydrological state is simplified and approximated, the computational power and time are restricted.

Nevertheless the results of the study report a plausible scenario concerning the hydrogeological characterization, the distribution of hydrological parameters and the vadose fluids mechanisms; crucial point for previsions and forecasting.

REFERENCES

- Allred B.J., Daniels J.J. and Ehsani M.R.; 2008: *Handbook of Agricultural Geophysics*. CRC Press, Taylor and Francis Group, New York.
- Alumbaugh D., Chang P.Y., Paprock L. I., Brainard I.R., Glass R.J. and Rautman C.A.; 2002: *Estimating moisture contents in the vadose zone using cross-borehole ground penetrating radar: A study of accuracy and repeatability*. Water Resources Research, **38** (12), 1309, doi: 10.1029/2001 WR000754.
- Annan A.P.; 2005: *GPR methods for hydrogeological studies*. In: Rubin Y. and Hubbard S.S. (ed.) Hydrogeophysics. Water Sci. Technol. Library Ser., **50**. Springer, New York, pp. 185–213.
- Archie G.E.; 1942: *The electrical resistivity log as an aid in determining some reservoir characteristics*: *Trans.AIME*, **146**, 54–62.
- Arcone S.A, 1984: *Field observations of electromagnetic pulse propagation in dielectric slabs*. Geophysics, **49** (10), 1763–1773. Arcone S.A., Peapples P.R., and Liu L.; 2003: *Propagation of a ground-penetrating radar (GPR) pulse in a thin surface waveguide*. Geophysics, **68** (3), 1922–1933.
- Bevc D. and H.F. Morrison; 1991: *Borehole-to-surface electrical resistivity monitoring of a salt water injection experiment*. Geophysics, **56** (6), 769–777.
- Besson A., Cousin I., Samouélian A., Boizard H. and Richard G.; 2004: *Structural heterogeneity of the soil tilled layer as characterized by 2D electrical resistivity surveying*. Soil & Tillage Research, **79**, 239–249
- Beven K.J. and Binley A.M.; 1992: *The future of distributed models: model calibration and uncertainty prediction*. Hydrological Processes, **6**, 279–298.
- Biegert E., Ferguson J. and Li X.; 2008: *4D gravity monitoring — Introduction*. Geophysics, **73** (6), Special Section – 4D gravity monitoring, WA1 (2008); doi:10.1190/1.3010377.

- Binley A., Henry-Poulter S. and Shaw B.; 1996: *Examination of solute transport in an undisturbed soil column using electrical resistance tomography*. Water Resources Research, **32**, 763–769.
- Binley A.M., Winship P., Middleton R. , Pokar M. and West J.; 2001: *High resolution characterization of vadose zone dynamics using cross-borehole radar*. Water Resources Research, **37**, 2639–2652.
- Binley A.M., Cassiani G., Middleton R. and Winship P.;2002a: *Vadose zone flow model parameterisation using cross-borehole radar and resistivity imaging*. Journal of Hydrology, **267**, 147-159.
- Binley A., Winship P., West L.J., Pokar M. and Middleton R.; 2002b: *Seasonal Variation of Moisture Content in Unsaturated Sandstone Inferred from Borehole Radar and Resistivity Profiles*. Journal of Hydrology, **267**, (3-4), 160-172.
- Binley A. and Beven K.; 2003: *Vadose zone flow model uncertainty as conditioned on geophysical data*. Ground Water, **41**, (2), 119-127.
- Binley A.M. and Kemna A. ; 2005: *DC resistivity and induced polarization methods*. In: Rubin Y. and Hubbard S.S. (ed.) Hydrogeophysics. Water Sci. Technol. Library Ser. **50**. Springer, New York pp. 129–156..
- Binley A.M., Slater L.D., Fukes M. and Cassiani G.; 2005: *The relationship between frequency dependent electrical resistivity and hydraulic properties of saturated and unsaturated sandstone*. Water Resources Research, **41**, (12), W12417 doi.org/10.1029/2005WR004202.
- Bohidar R.N. and Hermance J.F.; 2002: *The GPR refraction method*. Geophysics, **67**, (5), 1474–1485.
- Bras R.L. and Rodriguez-Iturbe I.; 1993: *Random functions and hydrology*. Dover publications, New York.

- Braun M, Kamm J. and Yaramanci U.; 2009: *Simultaneous inversion of magnetic resonance sounding in terms of water content, resistivity and decay times*. Near Surface Geophysics, **7**, (5-6), 589-598.
- Brovelli A., Cassiani G., Dalla E., Bergamini F., Pitea D. and Binley A.M.;2005: *Electrical properties of partially saturated sandstones: a novel computational approach with hydrogeophysical applications*. Water Resources Research, **41**, (8), W08411, doi/10.1029/2004WR003628.
- Brovelli A. and Cassiani G.; 2008: *Effective permittivity of porous media: a critical analysis of the Complex Refractive Index Model (CRIM)*. Geophysical Prospecting, **56**, 715–727, DOI: 10.1111/j. 1365-2478.2008.00724.x.
- Brovelli A. and Cassiani G.; 2010: *A combination of the Hashin-Shtrikman bounds aimed at modelling electrical conductivity and permittivity of variably saturated porous media*. Geophysical Journal International, **180**, 225-237, DOI: 10.1111/j.1365-246X.2009.04415.x.
- Cassiani G., Boehm G., Vesnaver A. and Nicolich R.; 1998: *A Geostatistical Framework for Incorporating Seismic Tomography Auxiliary Data into Hydraulic Conductivity Estimation*. Journal of Hydrology, **206**,(1-2), 58-74.
- Cassiani G., Strobbia C. and Gallotti L.; 2004: *Vertical Radar Profiles For The Characterization Of The Deep Vadose Zone*. Vadose Zone Journal, **3**, 1093-1115.
- Cassiani, G., Bruno, V., Villa, A., Fusi, N., Binley, A., 2006b. *A saline trace test monitored via time-lapse surface electrical resistivity tomography*. Journal of Applied Geophysics 59-3, 244-259.
- Cassiani G. and Binley A. M.; 2005: *Modeling Unsaturated Flow in a Layered Formation under Quasi-Steady State Conditions Using Geophysical Data Constraints*. Advances in Water Resources, **28**, (5), 467-477.
- Cassiani G., Binley A.M. and Ferré T.P.A.; 2006a: *Unsaturated zone processes*. In: Vereecken H. et

- al. (ed.) Applied Hydrogeophysics. NATO Sci. Ser., **71**, Springer-Verlag, Berlin, 75–116.
- Cassiani, G., Bruno, V., Villa, A., Fusi, N., Binley, A., 2006b. *A saline trace test monitored via time-lapse surface electrical resistivity tomography*. Journal of Applied Geophysics 59-3, 244-259.
- Cassiani G., Fusi N., Susanni D. and Deiana R.; 2008: *Vertical Radar Profiles for the assessment of landfill capping effectiveness*. Near Surface Geophysics, **6**, 133-142.
- Cassiani G., Godio A., Stocco S., Villa A., Deiana R., Frattini P. and Rossi M.; 2009a: *Monitoring the hydrologic behaviour of steep slopes via time-lapse electrical resistivity tomography*. Near Surface Geophysics, special issue on Hydrogeophysics, 475-486.
- Cassiani G., Ferraris S., Giustiniani M., Deiana R. and Strobbia C.; 2009b: *Time-lapse surface-to-surface GPR measurements to monitor a controlled infiltration experiment*. Bollettino di Geofisica Teorica ed Applicata, **50**, , 209-226.
- Chang P., Alumbaugh D., Brainard J. and Hall L.; 2006: *Cross-borehole ground-penetrating radar for monitoring and imaging solute transport within the vadose zone*. Water Resources Research, **42**, W10413. doi:10.1029/2004WR003871.
- Christiansen A.V., Auken E. and Sørensen K.; 2006: *The transient electromagnetic method*. In: Groundwater Geophysics: A Tool for Hydrogeology, R. Kirsch Ed., Springer.
- Crook N., Binley A., Knight R., Robinson D.A., Zarnetske J. and Haggerty R.; 2008: *Electrical Resistivity Imaging of the Architecture of Sub-Stream Sediments*. Water Resources Research, **44**, W00D13, doi:10.1029/2008WR006968.
- Daily W.D., Ramirez A.L., LaBrecque D.J. and Barber W.; 1995: *Electrical resistance tomography experiments at the Oregon Graduate Institute*. Journal of Applied Geophysics, **33**, 227–237.
- Daily W., Ramirez A., LaBrecque D. and Nitao J.; 1992: *Electrical resistivity tomography of vadose water movement*. Water Resouces Research, **28**, (5), 1429-1442.

- Dalla E., Cassiani G., Brovelli A., Pitea D.; 2004: *Electrical conductivity of unsaturated porous media: pore-scale models and comparison with laboratory data*. Geophysical Research Letters, **31**, (5), L05609 10.1029/2003GL019170 .
- Day-Lewis F.D., Lane J.W., Harris Jr. J.M. and Gorelick S.M.; 2003: *Time-lapse imaging of saline-tracer transport in fractured rock using difference-attenuation radar tomography*. Water Resources Research, **39**, 1290-1303, Doi: 10.1029/2002WR001722.
- Day-Lewis F.D. and Lane Jr. J.W.; 2004: *Assessing the resolution dependent utility of tomograms for geostatistics*. Geophysical Research Letters, **31**, L07503, doi:10.1029/2004GL019617.
- Day-Lewis F.D., Singha K. and Binley A.M.; 2005: *Applying petrophysical models to radar travel time and electrical resistivity tomograms: Resolution-dependent limitations*. Journal of Geophysical Research-Solid Earth, **110** (B8), B08206.
- Day-Lewis F.D. and Singha K.; 2008: *Geoelectrical inference of mass transfer parameters using temporal moments*. Water Resources Research, **44** (5), W05201.
- Deiana R., Cassiani G., Villa A., Bagliani A. and Bruno V.; 2008: *Model calibration of a water injection test in the vadose zone of the Po River plain using GPR cross-hole data*. Vadose Zone Journal, doi: 10.2136/vzj2006.0137,, 215-226.
- Deiana R., Cassiani G., Kemna A., Villa A., Bruno V. and Bagliani A.; 2007: *An experiment of non invasive characterization of the vadose zone via water injection and cross-hole time-lapse geophysical monitoring*. Near Surface Geophysics, **5**, 183-194.
- French H.K., Hardbattle C., Binley A., Winship P. and Jakobsen L.; 2002: *Monitoring snowmelt induced unsaturated flow and transport using electrical resistivity tomography*. Journal of Hydrology **267**, (3–4), 273–284.
- Giannopoulos A.; 2005: *Modelling ground penetrating radar by GprMax*. Construction and Building Materials, **19**, 755-762.
- Giustiniani M., Accaino F., Picotti S. and Tinivella U.; 2008: *Characterization of the shallow*

- aquifers by high-resolution seismic data*. Geophysical Prospecting, **56**, (5), 655-666.
- Grote K., Hubbard S. and Rubin Y.; 2003: *Field-scale estimation of volumetric water content using ground-penetrating-radar wave techniques*. Water Resources Research, **39**, (11), 1321, doi:10.1029/2003WR002045.
- Hubbard S.S., Peterson J.E., Majer Jr. E.L., Zawislanski P.T., Williams K.H., Roberts J. and Wobber F.; 1997: *Estimation of permeable pathways and water content using tomographic radar data*. Leading Edge, **16**, 1623–1628.
- Huisman J.A., Sperl C., Bouten W. and Verstraten J.M.; 2001: *Soil water content measurements at different scales: Accuracy of time domain reflectometry and ground-penetrating radar.*, *Journal of Hydrology*, **245**, 48–58.
- Huisman J.A., Hubbard S.S., Redman J.D. and Annan A.P.; 2003: *Measuring soil water content with ground penetrating radar: A review*. Vadose Zone Journal, **2**, 477–491.
- Huisman J.A., Rings J., Vrugt J.A., Sorg J. and Vereecken H.; 2010: *Hydraulic properties of a model dike from coupled Bayesian and multi-criteria hydrogeophysical inversion*. *Journal of Hydrology*, **380**, 62–73.
- Irving J., Knight R.; 2006: *Numerical modeling of ground-penetrating radar in 2-D using MATLAB*. *Computer & Geoscience*, **32**, 1247-1258.
- Johnson T.C., Routh P. S., Barrash W. and Knoll M. D.; 2007: *A field comparison of Fresnel zone and ray-based GPR attenuation-difference tomography for time-lapse imaging of electrically anomalous tracer or contaminant plumes*. *Geophysics*, **72**, (2), 21–29, doi 10.1190/1.2431638.
- Kelly W.E.; 1977: *Geoelectrical sounding for estimating hydraulic conductivity*. *Ground Water*, **15**, 420-425.
- Kemna A., Vanderborght J., Kulesa B. and Vereecken H.; 2002: *Imaging and characterisation of subsurface solute transport using electrical resistivity tomography (ERT) and equivalent transport models*. *Journal of Hydrology*, **267**, 125-146.

- Kemna A., Binley A. and Slater L.; 2004: *Cross-borehole IP imaging for engineering and environmental applications*. *Geophysics*, **69**, (1), 97-105.
- Kemna A., Binley A., Day-Lewis F., Englert A., Tezkan B., Vanderborght J., Vereecken H. and Winship P.; 2006: *Solute Transport Processes*, In: *Applied Hydrogeophysics*, Vereecken H. et al., eds., Springer-Verlag, Berlin.
- Kobr M., Mareš S. and Paillet F.; 2005: *Geophysical well logging. Borehole geophysics for hydrogeological studies: principles and applications*. In: Rubin Y. and Hubbard S.S. (eds) *Hydrogeophysics*, Springer.
- Koestel J., Kemna A., Javaux M., Binley A. and Vereecken H.; 2008: *Quantitative imaging of solute transport in an unsaturated and undisturbed soil monolith with 3D ERT and TDR*. *Water Resources Research*, **44**, W12411, doi:10.1029/2007WR006755.
- LeBlanc D.R., Garabedian S.P., Hess K.H., Gelhar L.W., Quadri R.D., Stollenwerk K.G. and Wood W.W.; 1991: *Large-scale natural gradient tracer test in sand and gravel, Cape Cod, Massachusetts, 1, Experimental design and observed tracer movement*. *Water Resources Research*, **27**, 895-910.
- LaBrecque D.J., Ramirez A. L., Daily W. D., Binley A. M. and Schima S. A.; 1996: *ERT Monitoring of Environmental Remediation Processes*, *Measurement Science and Technology*, **7**, (3), 375-383.
- Lesmes G. and Friedman S.; 2005: *Relationships between the electrical and hydrogeological properties of rocks and soils*. In: Rubin Y. and Hubbard S.S., eds., *Hydrogeophysics*, Springer, Dordrecht.
- Lin, H.J., Richards, D.R., Talbot, C.A., Yeh, G.T., Cheng, J. & Cheng, H. 1997. *FEMWATER: A Three-dimensional Finite Element Computer Model for Simulating Density-dependent Flow and Transport in Variably Saturated Media*. US Army Corps of Engineers and Pennsylvania State University Technical Report, CHL-97-12.

- Linde N., Binley A., Tryggvason A., Pedersen L. and Revil A.; 2006: *Improved hydrogeophysical characterization using joint inversion of crosshole electrical resistance and ground penetrating radar traveltime data*. Water Resources Research, **42**, (12), W04410, doi:10.1029/2004WR003806.
- Looms M.C., Binley A., Jensen K. H., Nielsen L. and Hansen T.M.; 2008a: *Identifying unsaturated hydraulic parameters using an integrated data fusion approach on cross-borehole geophysical data*. Vadose Zone Journal, **7**, 238-248.
- Looms M.C., Jensen K. H., Binley A. and Nielsen L.; 2008b: *Monitoring unsaturated flow and transport using geophysical methods*. Vadose Zone Journal, **7**, 227-237.
- Mavko G., Mukerji T. and Dvorkin J.; 2009: *The Rock Physics Handbook, 2nd edition*, Cambridge University Press.
- Mazác O., Kelly W.E. and Landa I.; 1985: *A hydrogeophysical model for relations between electrical and hydraulic properties of aquifers*. Journal of Hydrology, **79**, 1-19.
- Miller C.R., Routh P.S., Brosten T.R. and McNamara J.P.; 2008: *Application of timelapse ERT imaging to watershed characterization*. Geophysics **73**.
- Monego M., Cassiani G., Deiana R., Putti M., Passadore G. and Altissimo L.; 2010: *Tracer test in a shallow heterogeneous aquifer monitored via time-lapse surface ERT*. Geophysics, in press.
- Nash, J. E. and J. V. Sutcliffe ; 1970: *River flow forecasting through conceptual models part I — A discussion of principles*, Journal of Hydrology, **10** (3), 282–290.
- Naudet V., Revil A. and Bottero J. Y. and Bégassat P.; 2003: *Relationship between self-potential (SP) signals and redox conditions in contaminated groundwater*. Geophysical Research Letters, **30**, (21), 2091, doi:10.1029/2003GL018096.
- Ntarlagiannis D., Williams K.H., Slater L. and Hubbard S.; 2006: *Low-frequency electrical response to microbial induced sulfide precipitation*. Journal of Geophysical Research, **110**, G02009, doi:10.1029/2005JG000024.

- Nyquist J.E., Heaney M. J. and Toran L.; 2009: *Characterizing lakebed seepage and geologic heterogeneity using resistivity imaging and temperature measurements*. *Near Surface Geophysics*, **7**, 487-498.
- Parkin G., Redman D., von Bertoldi P. and Zhang Z.; 2000: *Measurement of soil water content below a wastewater trench using ground-penetrating radar*. *Water Resources Research*, **36**, (8), 2147-2154.
- Pellerin L., Holliger K. Slater L. and Yaramanci U.; 2009: *Special Issue on Hydrogeophysics – Methods and Processes, Foreword*. *Near Surface Geophysics*, **7**, (5-6), 303-305, doi: 10.3997/1873-0604.2009045.
- Petersen T. and Al Hagrey S.A.; 2009: *Mapping root zones of small plants using surface and borehole resistivity tomography*. *Leading Edge*, **10**, 1220-1224.
- Pollock D. and Cirpka O.A.; 2008: *Temporal moments in geoelectrical monitoring of salt tracer experiments*. *Water Resources Research*, **44**, (12), W12416.
- Ramirez A., Nitao J., Hanley W., Aines R., Glaser R., Sengupta S., Dyer K., Hickling T. and Daily W.; 2005: *Stochastic inversion of electrical resistivity changes using a Markov chain, Monte Carlo approach*. *Journal of Geophysical Research*, **110**, (B02101).
- Revil A., Naudet V., Nouzaret J. and Pessel M.; 2003: *Principles of electrography applied to self-potential electrokinetic sources and hydrogeological applications*. *Water Resources Research*, **39**, (5), 1114, doi:10.1029/2001WR000916.
- Robinson D.A. and Friedman S. P.; 2003: *A method for measuring the solid particle permittivity or electrical conductivity of rocks, sediments, and granular materials*. *Journal of Geophysical Research*, **108**, (B2, 2076).
- Robinson D.A., Binley A., Crook N., Day-Lewis F., Ferré P.T., Grauch V.J.S., Knight R., Knoll M., Lakshmi V., Miller R., Nyquist J., Pellerin L., Singha K. and Slater L.; 2007: *Advancing process-based watershed hydrological research using near-surface geophysics: A vision for,*

- and review of, electrical and magnetic geophysical methods*. Hydrological Processes, **22**, 3604-3635.
- Robinson D.A., Abdu H., Jones S.B., Seyfried M., Lebron I. and Knight R.; 2008: *Eco-Geophysical Imaging of Watershed-Scale Soil Patterns Links with Plant Community Spatial Patterns*. Vadose Zone Journal, **7**, 1132–1138.
- Rockhold ML, Simmons CS, Fayer MJ. *An analytical solution technique for one-dimensional, steady vertical water flow in layered soils*. Water Resour Res 1997;33(4):897–902.
- Roth K., Schulin R., Fluhler H. and Hattinger W.; 1990: *Calibration of time domain reflectometry for water content measurements using a composite dielectric approach*. Water Resources Research, **26**,(10), 2267-2273.
- Rubin Y.; 2003: *Applied Stochastic Hydrogeology*. Oxford University Press, New York.
- Rubin Y. and Hubbard S.S.; 2005: *Hydrogeophysics*, Springer eds, Dordrecht.
- Rucker D.F., Ferré T.P.A.; 2004: Correcting water content measurement errors associated with critically refracted first arrivals on zero offset profiling borehole ground penetrating radar profiles. Vadose Zone J., **3**, 278–287.
- Samouélian A., Richard G., Cousin I., Guerin R., Bruand A. and Tabbagh A.; 2004: *Three dimensional crack monitoring by electrical resistivity measurement*. European Journal of Soil Science, doi: 10.1111/j.1365-2389.2004.00632.x.
- Schlumberger, *Log Interpretation, Principles/Applications*, 1989.
- Schmalholz J., Stoffregen H., Kemna A. and Yaramanci U.; 2004: *Imaging of water content distributions inside a lysimeter using GPR tomography*. Vadose Zone Journal, **3**,1106–1115.
- Singha K., Pidlisecky A., Day-Lewis F.D. and Gooseff M.N.; 2008: *Electrical characterization of non-Fickian transport in groundwater and hyporheic systems*. Water Resources Research, **44**, W00D07.

- Singha K. and Gorelick S.M.; 2005: *Saline tracer visualized with three-dimensional electrical resistivity tomography: Field-scale spatial moment analysis*. Water Resources Research, **41**, (5), W05023.
- Singha K. and Gorelick S.M.; 2006a: *Hydrogeophysical tracking of three-dimensional tracer migration: The concept and application of apparent petrophysical relations*. Water Resources Research, **42**, (6), W06422.
- Singha K. and Gorelick S.M.; 2006b: *Effects of spatially variable resolution on field-scale estimates of tracer concentration from electrical inversions using Archie's law*. Geophysics, **71** (3), 83-91.
- Singha K. and Moysey S.; 2006: *Accounting for spatially variable resolution in electrical resistivity tomography through field-scale rock-physics relations*. Geophysics, **71**, (4), A25-A28.
- Slater L., Binley A. and Brown D.; 1997a: *Electrical imaging of fractures using ground-water salinity change*. Groundwater, **35**, 436–442.
- Slater L., Zaidman M.D., Binley A.M. and West L.J.; 1997b: *Electrical imaging of saline tracer migration for the investigation of unsaturated zone transport mechanisms*. Hydrology Earth System Sciences, **1**, 291–302.
- Slater L., Binley A.M., Daily W. and Johnson R.; 2000: *Cross-hole electrical imaging of a controlled saline tracer injection*. Journal of Applied Geophysics, **44**, 85-102.
- Slater L., Versteeg R., Binley A., Cassiani G., Birken R. and Sandberg S.; 2002: *A 3D ERT Study of Solute Transport in a Large Experimental Tank*. Journal of Applied Geophysics, **49**, 211-229.
- Slater L. and Binley A.; 2006: *Synthetic and field based electrical imaging of a zerovalent iron barrier: Implications for monitoring long-term barrier performance*. Geophysics, **71**, (5) ,B129-B137.
- Slater L.D.; 2007: *Near surface electrical characterization of hydraulic conductivity: From petrophysical properties to aquifer geometries - A review*. Surveys in Geophysics, **28**, (2-

3) ,169-197.

Strobbia C. and Cassiani G.; 2007: *Multi-layer GPR guided waves in shallow soil layers for the estimation of soil water content*. *Geophysics*, **72**, (4), J17–J29, 10.1190/1.2716374.

Sumner J.S.; 1976: *Principles of Induced Polarisation for Geophysical Exploration*. Elsevier, Amsterdam.

Suzuki K. and Higashi S.; 2001: *Groundwater flow after heavy rain in landslide-slope area from 2-D inversion of resistivity monitoring data*. *Geophysics*, **66**, (3), 733-743.

Topp G.C., Davis J.L. and Annan A.P.; 1980: *Electromagnetic determination of soil water content: measurements in coaxial transmission lines*. *Water Resources Research*, **16**, 574–582.

Topp G.C, Davis J.L. and Annan A.P.; 1982: *Electromagnetic determination of soil water content using TDR, 2: evaluation of installation and configuration of parallel transmission lines*. *Soil Sci. Soc. Am. J.*, **46**, (4), 678-684.

Topp G.C. and Davis J.L.; 1985: *Measurement of soil water content using Time Domain Reflectometry*. *Soil Sci. Soc. Am. J.* **49**, 19-24.

Uhlenbrook S., Wenninger J., Didszun J. and Tilch N.; 2008: *Use of electrical resistivity tomography (ERT) and tracers to explore flow pathways and residence times at the hillslope scale*. *Geophysical Research Abstracts*, **7**, 04948, 2005.

Vanderborght J., Kemna A., Hardelauf H. and Vereecken H.; 2005: *Potential of electrical resistivity tomography to infer aquifer transport characteristics from tracer studies: A synthetic case study*. *Water Resources Research*, **41**, W06013, doi: 10.1029/2004WR003774.

Van Genuchten, M.Th., 1980. *A closed-form equation for predicting the hydraulic conductivity of unsaturated soils*. *Soil Sci. Soc. Am. J.* **44**, 892–898.

Van der Kruk J., Streich R. and Green A.G.; 2006: *Properties of surface waveguides derived from separate and joint inversion of dispersive TE and TM GPR data*. *Geophysics*, **71**, K19-K29, 10.1190/1.268011.

- Van Egmond F.M., Dietrich P., Werban U. and Sauer U.; 2009: *iSOIL: exploring the soil as the basis for quality crop production and food security*. Quality Assurance and Safety of Crops & Foods. 117-120doi:10.1111/j.1757-837X.2009.00019.x .
- Van Overmeeren R.A., Sariowan S.V. and Gehrels J.C. ; 1997 : *Ground penetrating radar for determining volumetric soil water content: Results of comparative measurements at two test sites*. Journal of Hydrology, **197**,316–338.
- Vereecken H., Yaramanci U. and Kemna A.; 2002: *Non-invasive Methods in Hydrology*. Journal of Hydrology: Special Issue, **267**, (3-4), 175 pp.
- Vereecken H., Hubbard S., Binley A. and Ferre T.; 2004: *Hydrogeophysics: An introduction from the guest editors*. Vadose Zone Journal, **3**, (4), 1060-1062.
- Vereecken H., Binley A., Cassiani G., Kharkhordin I., Revil A. and Titov K.; 2006: *Applied Hydrogeophysics*, Springer-Verlag eds., Berlin.
- West, L.J., Huang, Y., Handley, K., 2001. *Dependence of Sandstone Dielectric Behaviour on Moisture Content and Lithology*, Proceedings of the Symposium on Applications of Geophysics to Engineering and Environmental Problems (SAGEEP2001), Environmental and Engineering Geophysical Society, Denver, CO.
- Winship P., Binley A., Gomez D.; 2006: Flow and transport in the unsaturated Sherwood Sandstone: characterization using cross-borehole geophysical methods. Geological Society, London, Special Publications, 263, 219–231.